
Revisiting Heterophily For Graph Neural Networks

Sitao Luan^{1,2}, Chenqing Hua^{1,2}, Qincheng Lu¹, Jiaqi Zhu¹, Mingde Zhao^{1,2}, Shuyuan Zhang^{1,2},

Xiao-Wen Chang¹, Doina Precup^{1,2,3}

{sitao.luan@mail, chenqing.hua@mail, qincheng.lu@mail, jiaqi.zhu@mail, mingde.zhao@mail, shuyuan.zhang@mail, chang@cs, dprecup@cs}.mcgill.ca

¹McGill University; ²Mila; ³DeepMind

Abstract

Graph Neural Networks (GNNs) extend basic Neural Networks (NNs) by using graph structures based on the relational inductive bias (homophily assumption). While GNNs have been commonly believed to outperform NNs in real-world tasks, recent work has identified a non-trivial set of datasets where their performance compared to NNs is not satisfactory. Heterophily has been considered the main cause of this empirical observation and numerous works have been put forward to address it. In this paper, we first revisit the widely used homophily metrics and point out that their consideration of only graph-label consistency is a shortcoming. Then, we study heterophily from the perspective of post-aggregation node similarity and define new homophily metrics, which are potentially advantageous compared to existing ones. Based on this investigation, we prove that some harmful cases of heterophily can be effectively addressed by local diversification operation. Then, we propose the Adaptive Channel Mixing (ACM), a framework to adaptively exploit aggregation, diversification and identity channels node-wisely to extract richer localized information for diverse node heterophily situations. ACM is more powerful than the commonly used uni-channel framework for node classification tasks on heterophilic graphs and is easy to be implemented in baseline GNN layers. When evaluated on 10 benchmark node classification tasks, ACM-augmented baselines consistently achieve significant performance gain, exceeding state-of-the-art GNNs on most tasks without incurring significant computational burden.

1 Introduction

Deep Neural Networks (NNs) [22] have revolutionized many machine learning areas, including image recognition [21], speech recognition [13] and natural language processing [2], due to their effectiveness in learning latent representations from Euclidean data. Recent research has shifted focus on non-Euclidean data [6], *e.g.*, relational data or graphs. Combining graph signal processing and convolutional neural networks [23], numerous Graph Neural Network (GNN) architectures have been proposed [38, 10, 15, 40, 19, 29], which empirically outperform traditional NNs on graph-based machine learning tasks such as node classification, graph classification, link prediction and graph generation, *etc.* GNNs are built on the homophily assumption [34]: connected nodes tend to share similar attributes with each other [14], which offers additional information besides node features. This relational inductive bias [3] is believed to be a key factor leading to GNNs’ superior performance over NNs’ in many tasks.

However, growing empirical evidence suggests that GNNs are not always advantageous compared to traditional NNs. In some cases, even simple Multi-Layer Perceptrons (MLPs) can outperform GNNs by a large margin on relational data [45, 28, 31, 8]. An important reason for this is believed to be the heterophily problem: the homophily assumption does not always hold, so connected nodes may in fact have different attributes. Heterophily has received lots of attention recently and an increasing number of models have been put forward to address this problem [45, 28, 31, 8, 44, 43, 32, 16, 24]. In this paper, we first show that by only considering graph-label consistency, existing homophily metrics

are not able to describe the effect of some cases of heterophily on aggregation-based GNNs. We propose a post-aggregation node similarity matrix, and based on it, we derive new homophily metrics, whose advantages are illustrated on synthetic graphs (Sec. 3). Then, we prove that diversification operation can help to address some harmful cases of heterophily (Sec. 4). Based on this, we propose the Adaptive Channel Mixing (ACM) GNN framework which augments uni-channel baseline GNNs, allowing them to exploit aggregation, diversification and identity channels adaptively, node-wisely and locally in each layer. ACM significantly boosts the performance of 3 uni-channel baseline GNNs by 2.04% \sim 27.5% for node classification tasks on 7 widely used benchmark heterophilic graphs, exceeding SOTA models (Sec. 6) on all of them. For 3 homophilic graphs, ACM-augmented GNNs can perform at least as well as the uni-channel baselines and are competitive compared with SOTA.

Contributions 1. To our knowledge, we are the first to analyze heterophily from post-aggregation node similarity perspective. 2. The proposed ACM framework is highly different from adaptive filterbank with multiple channels and existing GNNs for heterophily: 1) the traditional adaptive filterbank channels [39] uses a scalar weight for each filter and this weight is shared by all nodes. In contrast, ACM provides a mechanism so that different nodes can learn different weights to utilize information from different channels to account for diverse local heterophily; 2) Unlike existing methods that leverage the high-order filters and global property of high-frequency signals [45, 28, 8, 16] which require more computational resources, ACM successfully addresses heterophily by considering only the **nodewise local information adaptively**. 3. Unlike existing methods that try to facilitate learning filters with high expressive power [45, 44, 8, 16], ACM aims that, when given a filter with certain expressive power, we can extract richer information from additional channels in a certain way to address heterophily. This makes ACM more flexible and easier to be implemented.

2 Preliminaries

In this section, we introduce notation and background knowledge. We use **bold** font for vectors (*e.g.*, \mathbf{v}). Suppose we have an undirected connected graph $\mathcal{G} = (\mathcal{V}, \mathcal{E}, A)$, where \mathcal{V} is the node set with $|\mathcal{V}| = N$; \mathcal{E} is the edge set without self-loops; $A \in \mathbb{R}^{N \times N}$ is the symmetric adjacency matrix with $A_{i,j} = 1$ if $e_{ij} \in \mathcal{E}$, otherwise $A_{i,j} = 0$. Let D denote the diagonal degree matrix of \mathcal{G} , *i.e.*, $D_{i,i} = d_i = \sum_j A_{i,j}$. Let \mathcal{N}_i denote the neighborhood set of node i , *i.e.*, $\mathcal{N}_i = \{j : e_{ij} \in \mathcal{E}\}$. A graph signal is a vector $\mathbf{x} \in \mathbb{R}^N$ defined on \mathcal{V} , where \mathbf{x}_i is associated with node i . We also have a feature matrix $X \in \mathbb{R}^{N \times F}$, whose columns are graph signals and whose i -th row $X_{i,:}$ is a feature vector of node i . We use $Z \in \mathbb{R}^{N \times C}$ to denote the label encoding matrix, whose i -th row $Z_{i,:}$ is the one-hot encoding of the label of node i .

2.1 Graph Laplacian, Affinity Matrix and Variants

The (combinatorial) graph Laplacian is defined as $L = D - A$, which is Symmetric Positive Semi-Definite (SPSD) [9]. Its eigendecomposition is $L = U\Lambda U^T$, where the columns \mathbf{u}_i of $U \in \mathbb{R}^{N \times N}$ are orthonormal eigenvectors, namely the *graph Fourier basis*, $\Lambda = \text{diag}(\lambda_1, \dots, \lambda_N)$ with $\lambda_1 \leq \dots \leq \lambda_N$. These eigenvalues are also called *frequencies*.

In addition to L , some variants are also commonly used, *e.g.*, the symmetric normalized Laplacian $L_{\text{sym}} = D^{-1/2}LD^{-1/2} = I - D^{-1/2}AD^{-1/2}$ and the random walk normalized Laplacian $L_{\text{rw}} = D^{-1}L = I - D^{-1}A$. The graph Laplacian and its variants can be considered as high-pass filters for graph signals. The affinity (transition) matrices can be derived from the Laplacians, *e.g.*, $A_{\text{rw}} = I - L_{\text{rw}} = D^{-1}A$, $A_{\text{sym}} = I - L_{\text{sym}} = D^{-1/2}AD^{-1/2}$ and are considered to be low-pass filters [33]. Their eigenvalues satisfy $\lambda_i(A_{\text{rw}}) = \lambda_i(A_{\text{sym}}) = 1 - \lambda_i(L_{\text{sym}}) = 1 - \lambda_i(L_{\text{rw}}) \in (-1, 1]$. Applying the renormalization trick [19] to affinity and Laplacian matrices respectively leads to $\hat{A}_{\text{sym}} = \tilde{D}^{-1/2}\tilde{A}\tilde{D}^{-1/2}$ and $\hat{L}_{\text{sym}} = I - \hat{A}_{\text{sym}}$, where $\tilde{A} \equiv A + I$ and $\tilde{D} \equiv D + I$. The renormalized affinity matrix essentially adds a self-loop to each node in the graph, and is widely used in Graph Convolutional Network (GCN) [19] as follows:

$$Y = \text{softmax}(\hat{A}_{\text{sym}} \text{ReLU}(\hat{A}_{\text{sym}} X W_0) W_1) \quad (1)$$

where $W_0 \in \mathbb{R}^{F \times F_1}$ and $W_1 \in \mathbb{R}^{F_1 \times O}$ are learnable parameter matrices. GCNs can be trained by minimizing the following cross entropy loss

$$\mathcal{L} = -\text{trace}(Z^T \log Y) \quad (2)$$

where $\log(\cdot)$ is a component-wise logarithm operation. The random walk renormalized matrix $\hat{A}_{rw} = \tilde{D}^{-1}\tilde{A}$, which shares the same eigenvalues as \hat{A}_{sym} , can also be applied in GCN. The corresponding Laplacian is defined as $\hat{L}_{rw} = I - \hat{A}_{rw}$. The matrix \hat{A}_{rw} is essentially a random walk matrix and behaves as a mean aggregator that is applied in spatial-based GNNs [15, 14]. To bridge spectral and spatial methods, we use \hat{A}_{rw} in this paper.

2.2 Metrics of Homophily

The homophily metrics are defined by considering different relations between node labels and graph structures. There are three commonly used homophily metrics: edge homophily [1, 45], node homophily [35] and class homophily [26]¹, defined as follows:

$$\begin{aligned} H_{\text{edge}}(\mathcal{G}) &= \frac{|\{e_{uv} \mid e_{uv} \in \mathcal{E}, Z_{u,:} = Z_{v,:}\}|}{|\mathcal{E}|}, \quad H_{\text{node}}(\mathcal{G}) = \frac{1}{|\mathcal{V}|} \sum_{v \in \mathcal{V}} H_{\text{node}}^v = \frac{1}{|\mathcal{V}|} \sum_{v \in \mathcal{V}} \frac{|\{u \mid u \in \mathcal{N}_v, Z_{u,:} = Z_{v,:}\}|}{d_v}, \\ H_{\text{class}}(\mathcal{G}) &= \frac{1}{C-1} \sum_{k=1}^C \left[h_k - \frac{|\{v \mid Z_{v,k}=1\}|}{N} \right]_+, \quad h_k = \frac{\sum_{v \in \mathcal{V}} |\{u \mid Z_{v,k}=1, u \in \mathcal{N}_v, Z_{u,:} = Z_{v,:}\}|}{\sum_{v \in \{v \mid Z_{v,k}=1\}} d_v} \end{aligned} \quad (3)$$

where H_{node}^v is the local homophily value for node v ; $[a]_+ = \max(a, 0)$; h_k is the class-wise homophily metric [26]. All metrics are in the range of $[0, 1]$; a value close to 1 corresponds to strong homophily, while a value close to 0 indicates strong heterophily. $H_{\text{edge}}(\mathcal{G})$ measures the proportion of edges that connect two nodes in the same class; $H_{\text{node}}(\mathcal{G})$ evaluates the average proportion of edge-label consistency of all nodes; $H_{\text{class}}(\mathcal{G})$ tries to avoid sensitivity to imbalanced classes, which can make $H_{\text{edge}}(\mathcal{G})$ misleadingly large. The above definitions are all based on the **linear feature-independent graph-label consistency**. The inconsistency relation is implied to have a negative effect to the performance of GNNs. With this in mind, in the following section, we give an example to illustrate the shortcomings of the above metrics and propose new feature-independent metrics that are defined from post-aggregation node similarity perspective, which is novel.

3 Analysis of Heterophily

3.1 Motivation and Aggregation Homophily

Heterophily is widely believed to be harmful for message-passing based GNNs [45, 35, 8] because, intuitively, features of nodes in different classes will be falsely mixed, leading nodes to be indistinguishable [45]. Nevertheless, it is not always the case, *e.g.*, the bipartite graph² shown in Figure 1 is highly heterophilic according to the existing homophily metrics in equation 3, but after mean aggregation, the nodes in classes 1 and 2 just exchange colors and are still distinguishable³. This example tells us that, besides graph-label consistency, we need to study the relation between nodes after aggregation step.

To this end, we first define the post-aggregation node similarity matrix as follows:

$$S(\hat{A}, X) \equiv \hat{A}X(\hat{A}X)^T \in \mathbb{R}^{N \times N} \quad (4)$$

where $\hat{A} \in \mathbb{R}^{N \times N}$ denotes a general aggregation operator. $S(\hat{A}, X)$ is essentially the gram matrix that measures the similarity between each pair of aggregated node features.

Relationship Between $S(\hat{A}, X)$ and Gradient of SGC SGC [41] is one of the most simple but representative GNN models and its output can be written as:

$$Y = \text{softmax}(\hat{A}XW) = \text{softmax}(Y') \quad (5)$$

¹[26] did not name this homophily metric. We named it *class homophily* based on its definition.

²[32] use the same example but not to demonstrate the deficiency of homophily metrics.

³[8] also point out the insufficiency of H_{node} by examples to show that different graph typologies with the same $H_{\text{node}}(\mathcal{G})$ can carry different label information.

With the loss function in equation 2, after each gradient descent step, we have $\Delta W = \gamma \frac{d\mathcal{L}}{dW}$, where γ is the learning rate. The update of Y' is (see Appendix E for derivation):

$$\Delta Y' = \hat{A}X\Delta W = \gamma \hat{A}X \frac{d\mathcal{L}}{dW} \propto \hat{A}X \frac{d\mathcal{L}}{dW} = \hat{A}XX^T \hat{A}^T(Z - Y) = S(\hat{A}, X)(Z - Y) \quad (6)$$

where $Z - Y$ is the prediction error matrix. The update direction of the prediction for node i is essentially a weighted sum of the prediction error, *i.e.*, $\Delta(Y')_{i,:} = \sum_{j \in \mathcal{V}} [S(\hat{A}, X)]_{i,j}(Z - Y)_{j,:}$ and $[S(\hat{A}, X)]_{i,j}$ can be considered as the weights. Intuitively, a high similarity value $[S(\hat{A}, X)]_{i,j}$ means node i tends to be updated to the same class as node j . This indicates that $S(\hat{A}, X)$ is closely related to a single layer GNN model.

Based on the above definition and observation, we define the aggregation similarity score as follows.

Definition 1. *The aggregation similarity score is:*

$$S_{\text{agg}}(S(\hat{A}, X)) = \frac{1}{|\mathcal{V}|} \left| \left\{ v \mid \text{Mean}_u(\{S(\hat{A}, X)_{v,u} | Z_{u,:} = Z_{v,:}\}) \geq \text{Mean}_u(\{S(\hat{A}, X)_{v,u} | Z_{u,:} \neq Z_{v,:}\}) \right\} \right| \quad (7)$$

where $\text{Mean}_u(\{\cdot\})$ takes the average over u of a given multiset of values or variables.

$S_{\text{agg}}(S(\hat{A}, X))$ measures the proportion of nodes $v \in \mathcal{V}$ as which the average weights on the set of nodes in the same class (including v) is larger than that in other classes. In practice, we observe that in most datasets, we will have $S_{\text{agg}}(S(\hat{A}, X)) \geq 0.5$ ⁴. To make the metric range in [0,1], like existing metrics, we rescale equation 7 to the following modified aggregation similarity,

$$S_{\text{agg}}^M(S(\hat{A}, X)) = [2S_{\text{agg}}(S(\hat{A}, X)) - 1]_+ \quad (8)$$

In order to measure the consistency between labels and graph structures without considering node features and to make a fair comparison with the existing homophily metrics in equation 3, we define the graph (\mathcal{G}) aggregation (\hat{A}) homophily and its modified version⁵ as:

$$H_{\text{agg}}(\mathcal{G}) = S_{\text{agg}}(S(\hat{A}, Z)), \quad H_{\text{agg}}^M(\mathcal{G}) = S_{\text{agg}}^M(S(\hat{A}, Z)) \quad (9)$$

As the example shown in Figure 1, when $\hat{A} = \hat{A}_{\text{rw}}$, it is easy to see that $H_{\text{agg}}(\mathcal{G}) = H_{\text{agg}}^M(\mathcal{G}) = 1$ and other metrics are 0. Thus, this new metric reflects the fact that nodes in classes 1 and 2 are still highly distinguishable after aggregation, while other metrics mentioned before fail to capture such information and misleadingly give value 0. This shows the advantage of $H_{\text{agg}}(\mathcal{G})$ and $H_{\text{agg}}^M(\mathcal{G})$, which additionally exploit information from aggregation operator \hat{A} and the similarity matrix.

To comprehensively compare $H_{\text{agg}}^M(\mathcal{G})$ with the existing metrics on their ability to elucidate the influence of graph structure on GNN performance, we generate synthetic graphs with different homophily levels and evaluate SGC [41] and GCN [19] on them in the next subsection.

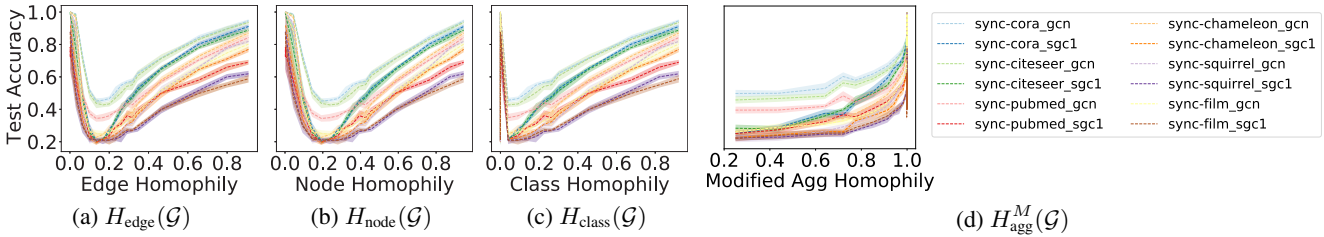


Figure 2: Comparison of baseline performance under different homophily metrics.

⁴See Appendix F.1 for an intuitive explanation under certain conditions.

⁵In practice, we will only check $H_{\text{agg}}(\mathcal{G})$ when $H_{\text{agg}}^M(\mathcal{G}) = 0$.

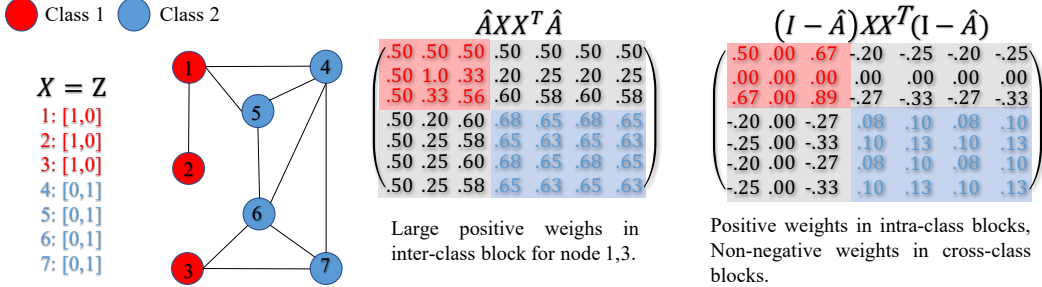


Figure 3: Example of how diversification can address harmful heterophily

3.2 Empirical Evaluation and Comparison on Synthetic Graphs

In this subsection, we conduct experiments on synthetic graphs generated with different levels of $H_{\text{edge}}^M(\mathcal{G})$ to assess the output of $H_{\text{agg}}^M(\mathcal{G})$ in comparison with existing metrics.

Data Generation & Experimental Setup We first generated 10 graphs for each of 28 edge homophily levels, from 0.005 to 0.95, for a total of 280 graphs. In every generated graph, we had 5 classes, with 400 nodes in each class. For nodes in each class, we randomly generated 800 intra-class edges and $[\frac{800}{H_{\text{edge}}(\mathcal{G})} - 800]$ inter-class edges. The features of nodes in each class are sampled from node features in the corresponding class of 6 base datasets (*Cora*, *CiteSeer*, *PubMed*, *Chameleon*, *Squirrel*, *Film*). Nodes were randomly split into train/validation/test sets, in proportion of 60%/20%/20%. We trained 1-hop SGC (*sgc-1*) [41] and GCN [19] on the synthetic graphs⁶. For each value of $H_{\text{edge}}(\mathcal{G})$, we take the average test accuracy and standard deviation of runs over the 10 generated graphs with that value. For each generated graph, we also calculate $H_{\text{node}}(\mathcal{G})$, $H_{\text{class}}(\mathcal{G})$ and $H_{\text{agg}}^M(\mathcal{G})$. Model performance with respect to different homophily values is shown in Figure 2.

Comparison of Homophily Metrics The performance of SGC-1 and GCN is expected to be monotonically increasing if the homophily metric is informative. However, Figure 2(a)(b)(c) show that the performance curves under $H_{\text{edge}}(\mathcal{G})$, $H_{\text{node}}(\mathcal{G})$ and $H_{\text{class}}(\mathcal{G})$ are U-shaped⁷, while Figure 2(d) reveals a nearly monotonic curve with a little numerical perturbation around 1. This indicates that $H_{\text{agg}}^M(\mathcal{G})$ provides a better indication of the way in which the graph structure affects the performance of SGC-1 and GCN than existing metrics. (See more discussion on aggregation homophily and theoretical results for regular graphs in Appendix D.)

4 Adaptive Channel Mixing (ACM)

In prior work [31, 8, 4], it has been shown that high-frequency graph signals, which can be extracted by a high-pass filter (HP), is empirically useful for addressing heterophily. In this section, based on the similarity matrix in equation 6, we theoretically prove that a diversification operation, *i.e.*, HP filter, can address some cases of harmful heterophily locally. Besides, a node-wise analysis shows that different nodes may need different filters to process their neighborhood information. Based on the above analysis, in Sec. 4.2 we propose Adaptive Channel Mixing (ACM), a 3-channel architecture which can adaptively exploit local and node-wise information from aggregation, diversification and identity channels.

4.1 Diversification Helps with Harmful Heterophily

We first consider the example shown in Figure 3. From $S(\hat{A}, X)$, we can see that nodes {1, 3} assign relatively large positive weights to nodes in class 2 after aggregation, which will make nodes {1, 3} hard to be distinguished from nodes in class 2. However, we can still distinguish nodes {1, 3} and {4, 5, 6, 7} by considering their neighborhood differences: nodes {1, 3} are different from most of their neighbors while nodes {4, 5, 6, 7} are similar to most of their neighbors. This indicates that

⁶See Appendix C.1 for a description of the hyperparameter searching range and Appendix D for more a detailed description of the data generation process

⁷A similar J-shaped curve for $H_{\text{edge}}(\mathcal{G})$ is found in [45], though using different data generation processes. The authors do not mention the insufficiency of edge homophily.

although some nodes become similar after aggregation, they are still distinguishable through their local surrounding dissimilarities.

This observation leads us to introduce the *diversification operation*, *i.e.*, HP filter $I - \hat{A}$ [11] to extract information regarding neighborhood differences, thereby addressing harmful heterophily. As $S(I - \hat{A}, X)$ in Fig. 3 shows, nodes $\{1, 3\}$ will assign negative weights to nodes $\{4, 5, 6, 7\}$ after the diversification operation, *i.e.*, nodes 1,3 treat nodes 4,5,6,7 as negative samples and will move away from them during backpropagation. This example reveals that there are cases in which the diversification operation is helpful to handle heterophily, while the aggregation operation is not. Based on this observation, we first define the diversification distinguishability of a node and the graph diversification distinguishability value, which measures the proportion of nodes for which the diversification operation is potentially helpful.

Definition 2. *Diversification Distinguishability (DD) based on $S(I - \hat{A}, X)$.*

Given $S(I - \hat{A}, X)$, a node v is diversification distinguishable if the following two conditions are satisfied at the same time,

1. $\text{Mean}_u \left(\{S(I - \hat{A}, X)_{v,u} | u \in \mathcal{V} \wedge Z_{u,:} = Z_{v,:}\} \right) \geq 0;$
2. $\text{Mean}_u \left(\{S(I - \hat{A}, X)_{v,u} | u \in \mathcal{V} \wedge Z_{u,:} \neq Z_{v,:}\} \right) \leq 0$

Then, graph diversification distinguishability value is defined as

$$\text{DD}_{\hat{A}, X}(\mathcal{G}) = \frac{1}{|\mathcal{V}|} \left| \{v | v \in \mathcal{V} \wedge v \text{ is diversification distinguishable}\} \right| \quad (11)$$

We can see that $\text{DD}_{\hat{A}, X}(\mathcal{G}) \in [0, 1]$. Based on Def. 2, the effectiveness of diversification in addressing heterophily can be theoretically proved under certain conditions:

Theorem 1. (See Appendix G for proof). For $C = 2$, suppose $X = Z, \hat{A} = \hat{A}_{\text{rw}}$. Then for any $I - \hat{A}_{\text{rw}}$, all nodes are diversification distinguishable and $\text{DD}_{\hat{A}, Z}(\mathcal{G}) = 1$.

With the above results for HP filters, we will now introduce the concept of filterbank which combines both LP (aggregation) and HP (diversification) filters and can potentially handle various local heterophily cases. We then develop ACM framework in the following subsection.

4.2 Filterbank and Adaptive Channel Mixing (ACM) Framework

Filterbank For the graph signal \mathbf{x} defined on \mathcal{G} , a 2-channel linear (analysis) filterbank [11]⁸ includes a pair of filters $H_{\text{LP}}, H_{\text{HP}}$, which retain the low-frequency and high-frequency content of \mathbf{x} , respectively. Most existing GNNs use a uni-channel filtering architecture [19, 40, 15] with either LP or HP channel, which only partially preserves the input information. Unlike the uni-channel architecture, filterbanks with $H_{\text{LP}} + H_{\text{HP}} = I$ do not lose any information from the input signal, which is called the perfect reconstruction property [11]. Generally, the Laplacian matrices ($L_{\text{sym}}, L_{\text{rw}}, \hat{L}_{\text{sym}}, \hat{L}_{\text{rw}}$) can be regarded as HP filters [11] and affinity matrices ($A_{\text{sym}}, A_{\text{rw}}, \hat{A}_{\text{sym}}, \hat{A}_{\text{rw}}$) can be treated as LP filters [33, 14]. Moreover, we extend the concept of filterbank and view MLPs as using the identity (full-pass) filterbank with $H_{\text{LP}} = I$ and $H_{\text{HP}} = 0$, which also satisfies $H_{\text{LP}} + H_{\text{HP}} = I + 0 = I$.

Node-wise Channel Mixing for Diverse Local Homophily The example in Figure 3 also shows that different nodes may need the local information extracted from different channels, *e.g.*, nodes $\{1, 3\}$ demand information from the HP channel while node 2 only needs information from the LP channel. Figure 4 reveals that nodes have diverse distributions of node local homophily H_{node}^v across different datasets. In order to adaptively leverage the LP, HP and identity channels in GNNs to deal with the diverse local heterophily situations, we will now describe our proposed Adaptive Channel Mixing (ACM) framework.

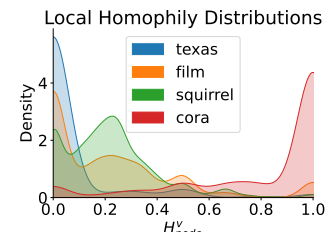


Figure 4: H_{node}^v distributions

⁸In graph signal processing, an additional synthesis filter [11] is required to form the 2-channel filterbank. But a synthesis filter is not needed in our framework.

Adaptive Channel Mixing (ACM) We will use GCN⁹ as an example to introduce the ACM framework in matrix form, but the framework can be combined in a similar manner to many different GNNs. The ACM framework includes the following steps:

Step 1. Feature Extraction for Each Channel:

$$\text{Option 1: } H_L^l = \text{ReLU}(H_{\text{LP}} H^{l-1} W_L^{l-1}), H_H^l = \text{ReLU}(H_{\text{HP}} H^{l-1} W_H^{l-1}), H_I^l = \text{ReLU}(I H^{l-1} W_I^{l-1});$$

$$\text{Option 2: } H_L^l = H_{\text{LP}} \text{ReLU}(H^{l-1} W_L^{l-1}), H_H^l = H_{\text{HP}} \text{ReLU}(H^{l-1} W_H^{l-1}), H_I^l = I \text{ReLU}(H^{l-1} W_I^{l-1});$$

$$H^0 = X \in \mathbb{R}^{N \times F_0}, W_L^{l-1}, W_H^{l-1}, W_I^{l-1} \in \mathbb{R}^{F_{l-1} \times F_l}, l = 1, \dots, L;$$

Step 2. Row-wise Feature-based Weight Learning

$$\tilde{\alpha}_L^l = \text{Sigmoid}(H_L^l \tilde{W}_L^l), \tilde{\alpha}_H^l = \text{Sigmoid}(H_H^l \tilde{W}_H^l), \tilde{\alpha}_I^l = \text{Sigmoid}(H_I^l \tilde{W}_I^l), \tilde{W}_L^{l-1}, \tilde{W}_H^{l-1}, \tilde{W}_I^{l-1} \in \mathbb{R}^{F_l \times 1}$$

$$[\alpha_L^l, \alpha_H^l, \alpha_I^l] = \text{Softmax}(([\tilde{\alpha}_L^l, \tilde{\alpha}_H^l, \tilde{\alpha}_I^l] / T) W_{\text{Mix}}^l) \in \mathbb{R}^{N \times 3}, T \in \mathbb{R} \text{ temperature}, W_{\text{Mix}}^l \in \mathbb{R}^{3 \times 3};$$

Step 3. Node-wise Adaptive Channel Mixing:

$$H^l = \text{ReLU}(\text{diag}(\alpha_L^l) H_L^l + \text{diag}(\alpha_H^l) H_H^l + \text{diag}(\alpha_I^l) H_I^l)$$

We will refer to the instantiation which uses option 1 in step 1 as ACM and to the one using option 2 as ACMII. In step 1, ACM(II)-GCN implement different feature extractions for 3 channels using a set of filterbanks. Three filtered components, H_L^l, H_H^l, H_I^l , are obtained. To adaptively exploit information from each channel, ACM(II)-GCN first extract nonlinear information from the filtered signals, then use W_{Mix}^l to learn which channel is important for each node, leading to the row-wise weight vectors $\alpha_L^l, \alpha_H^l, \alpha_I^l \in \mathbb{R}^{N \times 1}$ whose i -th elements are the weights for node i ¹⁰. These three vectors are then used as weights in defining the updated H^l in step 3.

Complexity The number of learnable parameters in layer l of ACM(II)-GCN is $3F_{l-1}(F_l + 1) + 9$, compared to $F_{l-1}F_l$ in GCN. The computation of steps 1-3 takes $NF_l(8 + 6F_{l-1}) + 2F_l(\text{nnz}(H_{\text{LP}}) + \text{nnz}(H_{\text{HP}})) + 18N$ flops, while the GCN layer takes $2NF_{l-1}F_l + 2F_l(\text{nnz}(H_{\text{LP}}))$ flops, where $\text{nnz}(\cdot)$ is the number of non-zero elements. An ablation study and a detailed comparison on running time are conducted in Sec. 6.1.

Limitations of Diversification Like any other method, there exists some cases of harmful heterophily that diversification operation cannot work well. For example, suppose we have an imbalanced dataset where several small clusters with distinctive labels are densely connected to a large cluster. In this case, the surrounding differences of nodes in small clusters are similar, *i.e.*, the neighborhood differences mainly come from their connections to the same large cluster, and this can lead to the diversification operation failing to discriminate them. See Appendix H for a more detailed discussion.

5 Related Work

We now discuss relevant work on addressing heterophily in GNNs. [1] acknowledges the difficulty of learning on graphs with weak homophily and propose MixHop to extract features from multi-hop neighborhoods to get more information. [17] propose measurements based on feature smoothness and label smoothness that are potentially helpful to guide GNNs when dealing with heterophilic graphs. Geom-GCN [35] precomputes unsupervised node embeddings and uses the graph structure defined by geometric relationships in the embedding space to define the bi-level aggregation process to handle heterophily. H₂GCN [45] combines 3 key designs to address heterophily: (1) ego- and neighbor-embedding separation; (2) higher-order neighborhoods; (3) combination of intermediate representations. CPGNN [44] models label correlations through a compatibility matrix, which is beneficial for heterophilic graphs, and propagates a prior belief estimation into the GNN by using the compatibility matrix. FAGCN [4] learns edge-level aggregation weights as GAT [40] but allows the weights to be negative, which enables the network to capture high-frequency components in the graph signals. GPRGNN [8] uses learnable weights that can be both positive and negative for feature propagation. This allows GPRGNN to adapt to heterophilic graphs and to handle both high- and low-frequency parts of the graph signals (See Appendix J for a more comprehensive comparison between ACM-GNNs, ACMII-GNNs and FAGCN, GPRGNN). BernNet [16] designs a scheme to learn arbitrary graph spectral filters with Bernstein polynomial to address heterophily. [32] points out that homophily is not necessary for GNNs and characterizes conditions that GNNs can perform well on heterophilic graphs.

⁹See more variants in Appendix B.

¹⁰See Appendix A.4 and A.5 for more discussion of the components in ACM architecture.

6 Empirical Evaluation

In this section, we evaluate the proposed ACM and ACMII framework on real-world datasets (see Appendix D.2 for a performance comparison with baseline models on synthetic datasets). We first conduct ablation studies in Sec. 6.1 to validate the effectiveness and efficiency of different components of ACM and ACMII. Then, we compare with state-of-the-art (SOTA) models in Sec. 6.2. The hyperparameter searching range and computing resources are described in Appendix C.

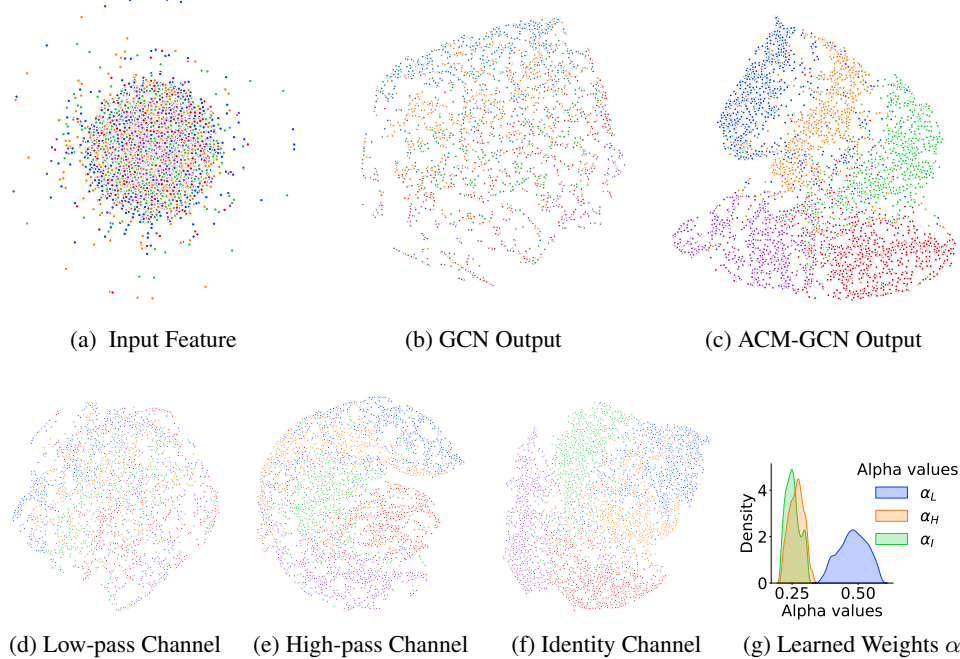


Figure 5: t-SNE visualization of the output layer of ACM-GCN and GCN trained on Squirrel

6.1 Ablation Study & Efficiency

We will now investigate the effectiveness and efficiency of adding HP, identity channels and the adaptive mixing mechanism in the proposed framework by performing an ablation study. Specifically, we apply the components of ACM to SGC-1 [41]¹¹ and the components of ACM and ACMII to GCN [19] separately. We run 10 times on each of the 9 benchmark datasets, *Cornell*, *Wisconsin*, *Texas*, *Film*, *Chameleon*, *Squirrel*, *Cora*, *CiteSeer* and *Pubmed* used in [36, 35], with the same 60%/20%/20% random splits for train/validation/test used in [8] and report the average test accuracy as well as the standard deviation. We also record the average running time per epoch (in milliseconds) to compare the computational efficiency. We set the temperature T in equation 4.2 to be 3, which is the number of channels.

The results in Table 1 show that on most datasets, the additional HP and identity channels are helpful, even for strong homophily datasets such as *Cora*, *CiteSeer* and *PubMed*. The adaptive mixing mechanism also has an advantage over directly adding the three channels together. This illustrates the necessity of learning to customize the channel usage adaptively for different nodes. The t-SNE visualization in Figure 5 demonstrates that the high-pass channel(e) and identity channel(f) can extract meaningful patterns, which the low-pass channel(d) is not able to capture. The output of ACM-GCN(c) shows clearer boundaries among classes than GCN(b). The running time is approximately doubled in the ACM and ACMII framework compared to the original models.

¹¹We only test ACM-SGC-1 because SGC-1 does not contain any non-linearity which makes ACM-SGC-1 and ACMII-SGC-1 exactly the same.

Ablation Study on Different Components in ACM-SGC and ACM-GCN (%)												
Baseline	Model Components		Cornell	Wisconsin	Texas	Film	Chameleon	Squirrel	Cora	CiteSeer	PubMed	Rank
Models	LP HP Identity Mixing		Acc \pm Std	Rank								
ACM-SGC-1 w/	✓		70.98 \pm 8.39	70.38 \pm 2.85	83.28 \pm 5.43	25.26 \pm 1.18	64.86 \pm 1.81	47.62 \pm 1.27	85.12 \pm 1.64	79.66 \pm 0.75	85.5 \pm 0.76	12.89
	✓	✓	83.28 \pm 5.81	91.88 \pm 1.61	90.98 \pm 2.46	36.76 \pm 1.01	65.27 \pm 1.9	47.27 \pm 1.37	86.8 \pm 1.08	80.98 \pm 1.68	87.21 \pm 0.42	10.44
	✓	✓	93.93 \pm 3.6	95.25 \pm 1.84	93.93 \pm 2.54	38.38 \pm 1.13	63.83 \pm 2.07	46.79 \pm 0.75	86.73 \pm 1.28	80.57 \pm 0.99	87.8 \pm 0.58	9.44
	✓	✓	88.2 \pm 4.39	93.5 \pm 2.95	92.95 \pm 2.94	37.19 \pm 0.87	62.82 \pm 1.84	44.94 \pm 0.93	85.22 \pm 1.35	80.75 \pm 1.68	88.11 \pm 0.21	11.00
ACM-GCN w/	✓	✓	93.77 \pm 1.91	93.25 \pm 2.92	93.61 \pm 1.55	39.33 \pm 1.25	63.68 \pm 1.62	46.4 \pm 1.13	86.63 \pm 1.13	80.96 \pm 0.93	87.75 \pm 0.88	10.00
	✓		82.46 \pm 3.11	75.5 \pm 2.92	83.11 \pm 3.2	35.51 \pm 0.99	64.18 \pm 2.62	44.76 \pm 1.39	87.78 \pm 0.96	81.39 \pm 1.23	88.9 \pm 0.32	11.44
	✓	✓	82.13 \pm 2.59	86.62 \pm 4.61	89.19 \pm 3.04	38.06 \pm 1.35	69.21 \pm 1.68	57.2 \pm 1.01	88.93 \pm 1.55	81.96 \pm 0.91	90.01 \pm 0.8	7.22
	✓	✓	94.26 \pm 2.23	96.13 \pm 2.2	94.1 \pm 2.95	41.51 \pm 0.99	67.44 \pm 2.14	53.97 \pm 1.39	88.95 \pm 0.9	81.72 \pm 1.22	90.88 \pm 0.55	4.44
ACMII-GCN w/	✓	✓	91.64 \pm 2	95.37 \pm 3.31	95.25 \pm 2.37	40.47 \pm 1.49	68.93 \pm 2.04	54.78 \pm 1.27	89.13 \pm 1.77	81.96 \pm 2.03	91.01 \pm 0.7	3.11
	✓	✓	94.75 \pm 2.62	96.75 \pm 1.6	95.08 \pm 3.2	41.62 \pm 1.15	69.04 \pm 1.74	58.02 \pm 1.86	88.95 \pm 1.3	81.80 \pm 1.26	90.69 \pm 0.53	2.78
	✓	✓	82.46 \pm 3.03	91.00 \pm 1.75	90.33 \pm 2.69	38.39 \pm 0.75	67.59 \pm 2.14	53.67 \pm 1.71	89.13 \pm 1.14	81.75 \pm 0.85	89.87 \pm 0.39	7.44
	✓	✓	94.26 \pm 2.57	96.00 \pm 2.15	94.26 \pm 2.96	40.96 \pm 1.2	66.35 \pm 1.76	50.78 \pm 2.07	89.06 \pm 1.07	81.86 \pm 1.22	90.71 \pm 0.67	4.67
ACMII-GCN w/	✓	✓	91.48 \pm 1.43	96.25 \pm 2.09	93.77 \pm 2.91	40.27 \pm 1.07	66.52 \pm 2.65	52.9 \pm 1.64	88.83 \pm 1.16	81.54 \pm 0.95	90.6 \pm 0.47	6.67
	✓	✓	95.9 \pm 1.83	96.62 \pm 2.44	95.25 \pm 3.15	41.84 \pm 1.15	68.38 \pm 1.36	54.53 \pm 2.09	89.00 \pm 0.72	81.79 \pm 0.95	90.74 \pm 0.5	2.78
Comparison of Average Running Time Per Epoch(ms)												
ACM-SGC-1 w/	✓		2.53	2.83	2.5	3.18	3.48	4.65	3.47	3.43	4.04	
	✓	✓	4.01	4.57	4.24	4.55	4.76	5.09	5.39	4.69	4.75	
	✓	✓	3.88	4.01	4.04	4.43	4.06	4.5	4.38	3.82	4.16	
	✓	✓	3.31	3.49	3.18	3.7	3.53	4.83	3.92	3.87	4.24	
ACM-GCN w/	✓	✓	5.53	5.96	5.43	5.21	5.41	6.96	6	5.9	6.04	
	✓	✓	3.67	3.74	3.59	4.86	4.96	6.41	4.24	4.18	5.08	
	✓	✓	6.63	8.06	7.89	8.11	7.8	9.39	7.82	7.38	8.74	
	✓	✓	5.73	5.91	5.93	6.86	6.35	7.15	7.34	6.65	6.8	
ACMII-GCN w/	✓	✓	5.16	5.25	5.2	5.93	5.64	8.02	5.73	5.65	6.16	
	✓	✓	8.25	8.11	7.89	7.97	8.41	11.9	8.84	8.38	8.63	
	✓	✓	6.62	7.35	7.39	7.62	7.33	9.69	7.49	7.58	7.97	
	✓	✓	6.3	6.05	6.26	6.87	6.44	6.5	6.14	7.21	6.6	
ACMII-GCN w/	✓	✓	5.24	5.27	5.46	5.72	5.65	7.87	5.48	5.65	6.33	
	✓	✓	7.59	8.28	8.06	8.85	8	10	8.27	8.5	8.68	

Table 1: Ablation study on 9 real-world datasets [35]. Cell with ✓ means the component is applied to the baseline model. The best test results are highlighted.

6.2 Comparison with Baseline and SOTA Models

Datasets & Experimental Setup In this section, we evaluate SGC [41] with 1 hop and 2 hops (SGC-1, SGC-2), GCNII [7], GCNII* [7], GCN [19] and snowball networks [29] with 2 and 3 layers (snowball-2, snowball-3) and combine them with the ACM or ACMII framework¹². We use \hat{A}_{rw} as the LP filter and the corresponding HP filter is $I - \hat{A}_{rw}$ ¹³. Both filters are deterministic. We compare these approaches with several baselines and SOTA GNN models: MLP with 2 layers (MLP-2), GAT [40], APPNP [20], GPRGNN [8], H₂GCN [45], MixHop [1], GCN+JK [19, 42, 26], GAT+JK [40, 42, 26], FAGCN [4], GraphSAGE [15], Geom-GCN [35] and BernNet [16]. In addition to the 9 benchmark datasets used in section 6.1, we further test the above models on a new benchmark dataset, *Deezer-Europe* [37]¹⁴.

On each dataset used in [36, 35], we test the models 10 times following the same early stopping strategy, the same 60%/20%/20% random data split¹⁵ and Adam [18] optimizer as used in GPRGNN [8]. For *Deezer-Europe*, we test the above models 5 times with the same early stopping strategy, the same fixed splits and Adam used in [26].

Structure information channel and residual connection Besides the filtered features, some recent SOTA models additionally use graph structure information, *i.e.*, $MLP_{\theta}(A)$, and residual connection to address heterophily problem, *e.g.*, LINKX [25] and GloGNN [24]. $MLP_{\theta}(A)$ and residual connection can be directly incorporated into ACM and ACMII framework, which leads us to ACM(II)-GCN+ and ACM(II)-GCN++. See the details of implementation in Appendix B.

To visualize the performance, in Fig. 6, we plot the bar charts of the test accuracy of SOTA models, three selected baselines (GCN, snowball-2, snowball-3), their ACM(II) augmented models, ACM(II)-

¹²GCNII and GCNII* are hard to implement with the ACMII framework. See Appendix B for explanation.

¹³See Appendix A.3 for the comparison of \hat{A}_{rw} and \hat{A}_{sym} .

¹⁴We choose *Deezer-Europe* because MLP outperforms GCN on it [26].

¹⁵See table 3 in Appendix A.2 for the performance comparison with several SOTA models, *e.g.*, LINKX [25] and GloGNN [24], on the fixed 48%/32%/20% splits provided by [35].

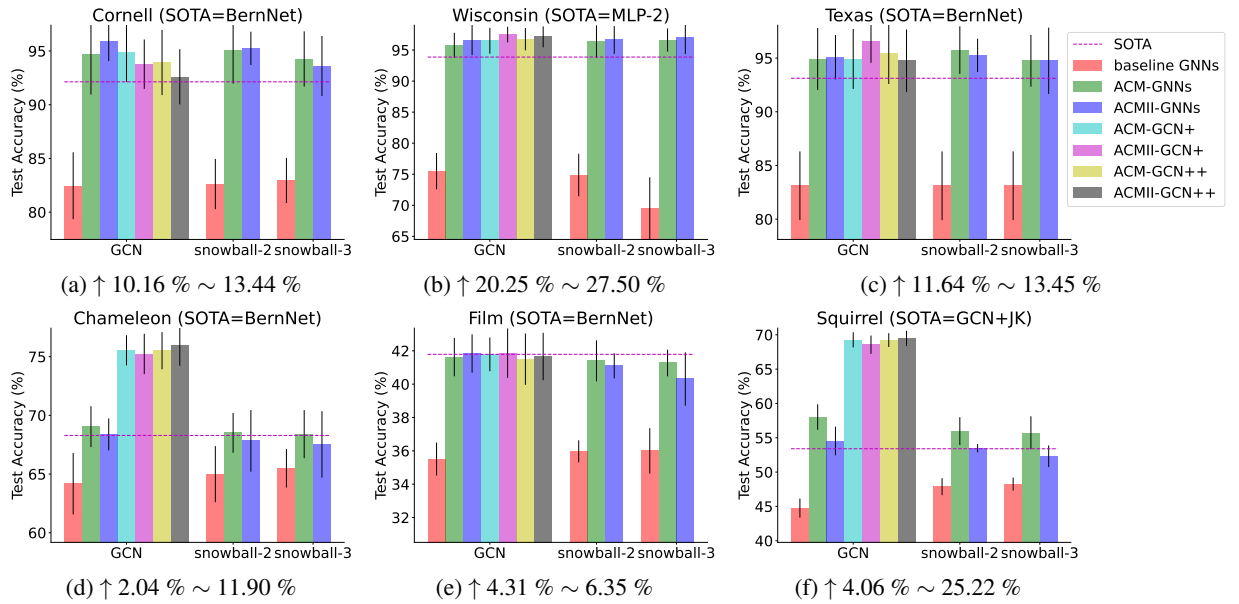


Figure 6: Comparison of baseline GNNs (red), ACM-GNNs (green), ACMII-GNNs (blue) with SOTA (magenta line) models on 6 selected datasets. The black lines indicate the standard deviation. The symbol “↑” shows the range of performance improvement (%) of ACM-GNNs and ACMII-GNNs over baseline GNNs. See Appendix I for a detailed discussion of the relation between H_{agg}^M and GNN performance.

GCN+ and ACM(II)-GCN++ on the 6 most commonly used benchmark heterophily datasets (See Table 2 in Appendix A.1 for the full results, comparison and ranking). From Fig. 6, we can see that (1) after being combined with the ACM or ACMII framework, the performance of the three baseline models is **significantly boosted**, by **2.04%~27.50%** on all the 6 tasks. The ACM and ACMII in fact achieve SOTA performance. (2) On *Cornell*, *Wisconsin*, *Texas*, *Chameleon* and *Squirrel*, the augmented baseline models **significantly outperform the current SOTA models**. Overall, these results suggest that the proposed approach can help GNNs to generalize better on node classification tasks on heterophilic graphs, without adding too much computational cost.

7 Conclusions and Limitations

We have presented an analysis of existing homophily metrics and proposed new metrics which are more informative in terms of correlating with GNN performance. To our knowledge, this is the first work analyzing heterophily from the perspective of post-aggregation node similarity. The similarity matrix and the new metrics we defined mainly capture linear feature-independent relationships of each node. This might be insufficient when nonlinearity and feature-dependent information is important for classification. In the future, it would be useful to investigate if a similarity matrix could be defined which is capable of capturing nonlinear and feature-dependent relations between aggregated node.

We have also proposed a multi-channel mixing mechanism which leverages the intuitions gained in the first part of the paper and can be combined with different GNN architectures, enabling adaptive filtering (high-pass, low-pass or identity) at different nodes. Empirically, this approach shows very promising results, improving the performance of the base GNNs with which it is combined and achieving SOTA results at the cost of a reasonable increase in computation time. As discussed in Sec. 4.2, however, the filterbank method cannot properly handle all cases of harmful heterophily, and alternative ideas should be explored as well in the future.

8 Acknowledge

The authors would like to give very special thanks to William L. Hamilton for valuable discussion and advice. The project was partially supported by DeepMind and NSERC.

References

- [1] S. Abu-El-Haija, B. Perozzi, A. Kapoor, N. Alipourfard, K. Lerman, H. Harutyunyan, G. Ver Steeg, and A. Galstyan. Mixhop: Higher-order graph convolutional architectures via sparsified neighborhood mixing. In *international conference on machine learning*, pages 21–29. PMLR, 2019.
- [2] D. Bahdanau, K. Cho, and Y. Bengio. Neural machine translation by jointly learning to align and translate. *arXiv preprint arXiv:1409.0473*, 2014.
- [3] P. W. Battaglia, J. B. Hamrick, V. Bapst, A. Sanchez-Gonzalez, V. Zambaldi, M. Malinowski, A. Tacchetti, D. Raposo, A. Santoro, R. Faulkner, et al. Relational inductive biases, deep learning, and graph networks. *arXiv preprint arXiv:1806.01261*, 2018.
- [4] D. Bo, X. Wang, C. Shi, and H. Shen. Beyond low-frequency information in graph convolutional networks. *arXiv preprint arXiv:2101.00797*, 2021.
- [5] C. Bodnar, F. Di Giovanni, B. P. Chamberlain, P. Liò, and M. M. Bronstein. Neural sheaf diffusion: A topological perspective on heterophily and oversmoothing in gnns. *arXiv preprint arXiv:2202.04579*, 2022.
- [6] M. M. Bronstein, J. Bruna, Y. LeCun, A. Szlam, and P. Vandergheynst. Geometric deep learning: going beyond euclidean data. *arXiv*, abs/1611.08097, 2016.
- [7] M. Chen, Z. Wei, Z. Huang, B. Ding, and Y. Li. Simple and deep graph convolutional networks. In *International Conference on Machine Learning*, pages 1725–1735. PMLR, 2020.
- [8] E. Chien, J. Peng, P. Li, and O. Milenkovic. Adaptive universal generalized pagerank graph neural network. In *International Conference on Learning Representations*. <https://openreview.net/forum>, 2021.
- [9] F. R. Chung and F. C. Graham. *Spectral graph theory*. Number 92. American Mathematical Soc., 1997.
- [10] M. Defferrard, X. Bresson, and P. Vandergheynst. Convolutional neural networks on graphs with fast localized spectral filtering. *arXiv*, abs/1606.09375, 2016.
- [11] V. N. Ekm̄baram. *Graph structured data viewed through a fourier lens*. University of California, Berkeley, 2014.
- [12] M. Fey and J. E. Lenssen. Fast graph representation learning with pytorch geometric. *arXiv preprint arXiv:1903.02428*, 2019.
- [13] A. Graves, A.-r. Mohamed, and G. Hinton. Speech recognition with deep recurrent neural networks. In *2013 IEEE international conference on acoustics, speech and signal processing*, pages 6645–6649. Ieee, 2013.
- [14] W. L. Hamilton. Graph representation learning. *Synthesis Lectures on Artificial Intelligence and Machine Learning*, 14(3):1–159, 2020.
- [15] W. L. Hamilton, R. Ying, and J. Leskovec. Inductive representation learning on large graphs. *arXiv*, abs/1706.02216, 2017.
- [16] M. He, Z. Wei, H. Xu, et al. Bernnet: Learning arbitrary graph spectral filters via bernstein approximation. *Advances in Neural Information Processing Systems*, 34, 2021.
- [17] Y. Hou, J. Zhang, J. Cheng, K. Ma, R. T. Ma, H. Chen, and M.-C. Yang. Measuring and improving the use of graph information in graph neural networks. In *International Conference on Learning Representations*, 2019.
- [18] D. P. Kingma and J. Ba. Adam: A method for stochastic optimization. *arXiv preprint arXiv:1412.6980*, 2014.
- [19] T. N. Kipf and M. Welling. Semi-supervised classification with graph convolutional networks. *arXiv*, abs/1609.02907, 2016.
- [20] J. Klicpera, A. Bojchevski, and S. Günnemann. Predict then propagate: Graph neural networks meet personalized pagerank. *arXiv preprint arXiv:1810.05997*, 2018.
- [21] A. Krizhevsky, I. Sutskever, and G. E. Hinton. Imagenet classification with deep convolutional neural networks. In *Advances in neural information processing systems*, pages 1097–1105, 2012.

[22] Y. LeCun, Y. Bengio, and G. Hinton. Deep learning. *nature*, 521(7553):436, 2015.

[23] Y. LeCun, L. Bottou, Y. Bengio, P. Haffner, et al. Gradient-based learning applied to document recognition. *Proceedings of the IEEE*, 86(11):2278–2324, 1998.

[24] X. Li, R. Zhu, Y. Cheng, C. Shan, S. Luo, D. Li, and W. Qian. Finding global homophily in graph neural networks when meeting heterophily. *arXiv preprint arXiv:2205.07308*, 2022.

[25] D. Lim, F. Hohne, X. Li, S. L. Huang, V. Gupta, O. Bhalerao, and S. N. Lim. Large scale learning on non-homophilous graphs: New benchmarks and strong simple methods. *Advances in Neural Information Processing Systems*, 34:20887–20902, 2021.

[26] D. Lim, X. Li, F. Hohne, and S.-N. Lim. New benchmarks for learning on non-homophilous graphs. *arXiv preprint arXiv:2104.01404*, 2021.

[27] V. Lingam, R. Ragesh, A. Iyer, and S. Sellamanickam. Simple truncated svd based model for node classification on heterophilic graphs. *arXiv preprint arXiv:2106.12807*, 2021.

[28] M. Liu, Z. Wang, and S. Ji. Non-local graph neural networks. *IEEE Transactions on Pattern Analysis and Machine Intelligence*, 2021.

[29] S. Luan, M. Zhao, X.-W. Chang, and D. Precup. Break the ceiling: Stronger multi-scale deep graph convolutional networks. *arXiv preprint arXiv:1906.02174*, 2019.

[30] S. Luan, M. Zhao, X.-W. Chang, and D. Precup. Training matters: Unlocking potentials of deeper graph convolutional neural networks. *arXiv preprint arXiv:2008.08838*, 2020.

[31] S. Luan, M. Zhao, C. Hua, X.-W. Chang, and D. Precup. Complete the missing half: Augmenting aggregation filtering with diversification for graph convolutional networks. *arXiv preprint arXiv:2008.08844*, 2020.

[32] Y. Ma, X. Liu, N. Shah, and J. Tang. Is homophily a necessity for graph neural networks? *arXiv preprint arXiv:2106.06134*, 2021.

[33] T. Maehara. Revisiting graph neural networks: All we have is low-pass filters. *arXiv preprint arXiv:1905.09550*, 2019.

[34] M. McPherson, L. Smith-Lovin, and J. M. Cook. Birds of a feather: Homophily in social networks. *Annual review of sociology*, 27(1):415–444, 2001.

[35] H. Pei, B. Wei, K. C.-C. Chang, Y. Lei, and B. Yang. Geom-gcn: Geometric graph convolutional networks. *arXiv preprint arXiv:2002.05287*, 2020.

[36] B. Rozemberczki, C. Allen, and R. Sarkar. Multi-Scale Attributed Node Embedding. *Journal of Complex Networks*, 9(2), 2021.

[37] B. Rozemberczki and R. Sarkar. Characteristic Functions on Graphs: Birds of a Feather, from Statistical Descriptors to Parametric Models. In *Proceedings of the 29th ACM International Conference on Information and Knowledge Management (CIKM '20)*, page 1325–1334. ACM, 2020.

[38] F. Scarselli, M. Gori, A. C. Tsoi, M. Hagenbuchner, and G. Monfardini. The graph neural network model. *IEEE transactions on neural networks*, 20(1):61–80, 2008.

[39] P. Vary. An adaptive filter-bank equalizer for speech enhancement. *Signal Processing*, 86(6):1206–1214, 2006.

[40] P. Velickovic, G. Cucurull, A. Casanova, A. Romero, P. Lio, and Y. Bengio. Graph attention networks. *arXiv*, abs/1710.10903, 2017.

[41] F. Wu, T. Zhang, A. H. d. Souza Jr, C. Fifty, T. Yu, and K. Q. Weinberger. Simplifying graph convolutional networks. *arXiv preprint arXiv:1902.07153*, 2019.

[42] K. Xu, C. Li, Y. Tian, T. Sonobe, K.-i. Kawarabayashi, and S. Jegelka. Representation learning on graphs with jumping knowledge networks. In J. Dy and A. Krause, editors, *Proceedings of the 35th International Conference on Machine Learning*, volume 80 of *Proceedings of Machine Learning Research*, pages 5453–5462. PMLR, 10–15 Jul 2018.

[43] Y. Yan, M. Hashemi, K. Swersky, Y. Yang, and D. Koutra. Two sides of the same coin: Heterophily and oversmoothing in graph convolutional neural networks. *arXiv preprint arXiv:2102.06462*, 2021.

[44] J. Zhu, R. A. Rossi, A. Rao, T. Mai, N. Lipka, N. K. Ahmed, and D. Koutra. Graph neural networks with heterophily. *arXiv preprint arXiv:2009.13566*, 2020.

[45] J. Zhu, Y. Yan, L. Zhao, M. Heimann, L. Akoglu, and D. Koutra. Beyond homophily in graph neural networks: Current limitations and effective designs. *Advances in Neural Information Processing Systems*, 33, 2020.

Checklist

1. For all authors...
 - (a) Do the main claims made in the abstract and introduction accurately reflect the paper's contributions and scope? **[Yes]**
 - (b) Did you describe the limitations of your work? **[Yes]**
 - (c) Did you discuss any potential negative societal impacts of your work? **[N/A]**
 - (d) Have you read the ethics review guidelines and ensured that your paper conforms to them? **[Yes]**
2. If you are including theoretical results...
 - (a) Did you state the full set of assumptions of all theoretical results? **[Yes]**
 - (b) Did you include complete proofs of all theoretical results? **[Yes]**
3. If you ran experiments...
 - (a) Did you include the code, data, and instructions needed to reproduce the main experimental results (either in the supplemental material or as a URL)? **[Yes]**
 - (b) Did you specify all the training details (e.g., data splits, hyperparameters, how they were chosen)? **[Yes]**
 - (c) Did you report error bars (e.g., with respect to the random seed after running experiments multiple times)? **[Yes]**
 - (d) Did you include the total amount of compute and the type of resources used (e.g., type of GPUs, internal cluster, or cloud provider)? **[Yes]**
4. If you are using existing assets (e.g., code, data, models) or curating/releasing new assets...
 - (a) If your work uses existing assets, did you cite the creators? **[Yes]**
 - (b) Did you mention the license of the assets? **[N/A]**
 - (c) Did you include any new assets either in the supplemental material or as a URL? **[No]**
 - (d) Did you discuss whether and how consent was obtained from people whose data you're using/curating? **[No]**
 - (e) Did you discuss whether the data you are using/curating contains personally identifiable information or offensive content? **[No]**
5. If you used crowdsourcing or conducted research with human subjects...
 - (a) Did you include the full text of instructions given to participants and screenshots, if applicable? **[N/A]**
 - (b) Did you describe any potential participant risks, with links to Institutional Review Board (IRB) approvals, if applicable? **[N/A]**
 - (c) Did you include the estimated hourly wage paid to participants and the total amount spent on participant compensation? **[N/A]**

A More Experimental Results

A.1 Comparison with SOTA Models on 60%/20%/20% Random Splits

The main results of the full sets of experiments ¹⁶ with statistics of datasets are summarized in Table 2, where we report the mean accuracy (%) and standard deviation. We can see that after applied in ACM or ACMII framework, the performance of baseline models are boosted on almost all tasks and achieve SOTA performance on 9 out of 10 datasets. Especially, ACMII-GCN+ performs the best in terms of average rank (4.40) across all datasets. Overall, It suggests that ACM or ACMII framework can significantly increase the performance of GNNs on node classification tasks on heterophilic graphs and maintain highly competitive performance on homophilic datasets.

	Cornell	Wisconsin	Texas	Film	Chameleon	Squirrel	Deezer-Europe	Cora	CiteSeer	PubMed	
#nodes	183	251	183	7,600	2,277	5,201	28,281	2,708	3,327	19,717	
#edges	295	499	309	33,544	36,101	217,073	92,752	5,429	4,732	44,338	
#features	1,703	1,703	1,703	931	2,325	2,089	31,241	1,433	3,703	500	
#classes	5	5	5	5	5	5	2	7	6	3	
H_{edge}	0.5669	0.4480	0.4106	0.3750	0.2795	0.2416	0.5251	0.8100	0.7362	0.8024	
H_{node}	0.3855	0.1498	0.0968	0.2210	0.2470	0.2156	0.5299	0.8252	0.7175	0.7924	
H_{class}	0.0468	0.0941	0.0013	0.0110	0.0620	0.0254	0.0304	0.7657	0.6270	0.6641	
Data Splits	60%/20%/20%	60%/20%/20%	60%/20%/20%	60%/20%/20%	60%/20%/20%	60%/20%/20%	60%/20%/20%	50%/25%/25%	60%/20%/20%	60%/20%/20%	
$H_{\text{agg}}^M(G)$	0.8032	0.7768	0.694	0.6822	0.61	0.3566	0.5790	0.9904	0.9826	0.9432	
	Test Accuracy (%) of State-of-the-art Models, Baseline GNN Models and ACM-GNN models										Rank
MLP-2	91.30 \pm 0.70	93.87 \pm 3.33	92.26 \pm 0.71	38.58 \pm 0.25	46.72 \pm 0.46	31.28 \pm 0.27	66.55 \pm 0.72	76.44 \pm 0.30	76.25 \pm 0.28	86.43 \pm 0.13	23.40
GAT	76.00 \pm 1.01	71.01 \pm 4.66	78.87 \pm 0.86	35.98 \pm 0.23	63.9 \pm 0.46	42.72 \pm 0.33	61.09 \pm 0.77	76.70 \pm 0.42	67.20 \pm 0.46	83.28 \pm 0.12	26.20
APPNP	91.80 \pm 0.63	92.00 \pm 3.59	91.18 \pm 0.70	38.86 \pm 0.24	51.91 \pm 0.56	34.77 \pm 0.34	67.21 \pm 0.56	79.41 \pm 0.38	68.59 \pm 0.30	85.02 \pm 0.09	22.80
GPRGNN	91.36 \pm 0.70	93.75 \pm 2.37	92.92 \pm 0.61	39.30 \pm 0.27	67.48 \pm 0.40	49.93 \pm 0.53	66.90 \pm 0.50	79.51 \pm 0.36	67.63 \pm 0.38	85.07 \pm 0.09	19.20
H2GCN	86.23 \pm 4.71	87.5 \pm 1.77	85.90 \pm 3.53	38.85 \pm 1.17	52.30 \pm 0.48	30.39 \pm 1.22	67.22 \pm 0.90	87.52 \pm 0.61	79.97 \pm 0.69	87.78 \pm 0.28	21.80
MixHop	60.33 \pm 28.53	77.25 \pm 7.80	76.39 \pm 7.66	33.13 \pm 2.40	36.28 \pm 10.22	24.55 \pm 2.60	66.80 \pm 0.58	65.65 \pm 11.31	49.52 \pm 13.35	87.04 \pm 4.10	28.30
GCN+JK	66.56 \pm 13.82	62.50 \pm 15.75	80.66 \pm 1.91	32.72 \pm 2.62	64.68 \pm 2.85	53.40 \pm 1.90	60.99 \pm 0.14	86.90 \pm 1.51	73.77 \pm 1.85	90.09 \pm 0.68	23.40
GAT+JK	74.43 \pm 10.24	69.50 \pm 3.12	75.41 \pm 7.18	35.41 \pm 0.97	68.14 \pm 1.18	52.28 \pm 3.61	59.66 \pm 0.92	89.52 \pm 0.43	74.49 \pm 2.76	89.15 \pm 0.87	20.90
FAGCN	88.03 \pm 5.6	89.75 \pm 6.37	88.85 \pm 4.39	31.59 \pm 1.37	49.47 \pm 2.84	42.24 \pm 1.2	66.86 \pm 0.53	88.85 \pm 1.36	82.37 \pm 1.46	89.98 \pm 0.54	18.20
BernNet	92.13 \pm 1.64	NA	93.12 \pm 0.65	41.79 \pm 1.01	68.29 \pm 1.58	51.35 \pm 0.73	NA	88.52 \pm 0.95	80.09 \pm 0.79	88.48 \pm 0.41	14.75
GraphSAGE	71.41 \pm 1.24	64.85 \pm 5.14	79.03 \pm 1.20	36.37 \pm 0.21	62.15 \pm 0.42	41.26 \pm 0.26	OOM	86.58 \pm 0.26	78.24 \pm 0.30	86.85 \pm 0.11	25.78
Geom-GCN*	60.81	64.12	67.57	31.63	60.9	38.14	NA	85.27	77.99	90.05	27.44
SGC-1	70.98 \pm 8.39	70.38 \pm 2.85	83.28 \pm 5.43	25.26 \pm 1.18	64.86 \pm 1.81	47.62 \pm 1.27	59.73 \pm 0.12	85.12 \pm 1.64	79.66 \pm 0.75	85.5 \pm 0.76	24.90
SGC-2	72.62 \pm 9.92	74.75 \pm 2.89	81.31 \pm 3.3	28.81 \pm 1.11	62.67 \pm 2.41	41.25 \pm 1.4	61.56 \pm 0.51	85.48 \pm 1.48	80.75 \pm 1.15	85.36 \pm 0.52	25.40
GCNII	89.18 \pm 3.96	83.25 \pm 2.69	82.46 \pm 4.58	40.82 \pm 1.79	60.35 \pm 2.7	38.81 \pm 1.97	66.38 \pm 0.45	88.98 \pm 1.33	81.58 \pm 1.3	89.8 \pm 0.3	19.30
GCNII*	90.49 \pm 4.45	89.12 \pm 3.06	88.52 \pm 3.02	41.54 \pm 0.99	62.8 \pm 2.87	38.31 \pm 1.3	66.42 \pm 0.56	88.93 \pm 1.37	81.83 \pm 1.78	89.98 \pm 0.52	16.40
GCN	82.46 \pm 3.11	75.5 \pm 2.92	83.11 \pm 3.2	35.51 \pm 0.99	64.18 \pm 2.62	44.76 \pm 1.39	62.23 \pm 0.53	87.78 \pm 0.96	81.39 \pm 1.23	88.9 \pm 0.32	20.90
Snowball-2	82.62 \pm 2.34	74.88 \pm 3.42	83.11 \pm 3.2	35.97 \pm 0.66	64.99 \pm 2.39	47.88 \pm 1.23	OOM	88.64 \pm 1.15	81.53 \pm 1.71	89.04 \pm 0.49	19.78
Snowball-3	82.95 \pm 2.1	69.5 \pm 5.01	83.11 \pm 3.2	36.00 \pm 1.36	65.49 \pm 1.64	48.25 \pm 0.94	OOM	89.33 \pm 1.3	80.93 \pm 1.32	88.8 \pm 0.82	19.11
ACM-SGC-1	93.77 \pm 1.91	93.25 \pm 2.92	93.61 \pm 1.55	39.33 \pm 1.25	63.68 \pm 1.62	46.4 \pm 1.13	66.67 \pm 0.56	86.63 \pm 1.13	80.96 \pm 0.93	87.75 \pm 0.88	17.00
ACM-SGC-2	93.77 \pm 2.17	94.00 \pm 2.61	93.44 \pm 2.54	40.13 \pm 1.21	60.48 \pm 1.55	40.91 \pm 1.39	66.53 \pm 0.57	87.64 \pm 0.99	80.93 \pm 1.16	88.79 \pm 0.5	17.70
ACM-GCNII	92.62 \pm 3.13	94.63 \pm 2.96	92.46 \pm 1.97	41.37 \pm 1.37	58.73 \pm 2.52	40.9 \pm 1.58	66.39 \pm 0.56	89.1 \pm 1.61	82.28 \pm 1.12	90.12 \pm 0.4	14.30
ACM-GCNII*	94.44 \pm 2.74	94.37 \pm 2.81	93.28 \pm 2.79	41.27 \pm 1.24	61.66 \pm 2.29	38.32 \pm 1.5	66.6 \pm 0.57	89.00 \pm 1.35	81.69 \pm 1.25	90.18 \pm 0.51	14.20
ACM-GCN	94.75 \pm 3.8	95.75 \pm 2.03	94.92 \pm 2.88	41.62 \pm 1.15	69.04 \pm 1.74	58.02 \pm 1.86	67.01 \pm 0.38	88.62 \pm 1.22	81.68 \pm 0.97	90.66 \pm 0.47	7.90
ACM-GCN+	94.92 \pm 2.79	96.5 \pm 2.08	94.92 \pm 2.79	41.79 \pm 1.01	76.08 \pm 2.13	69.26 \pm 1.11	67.4 \pm 0.44	89.75 \pm 1.16	81.65 \pm 1.48	90.46 \pm 0.69	4.90
ACM-GCN++	93.93 \pm 1.05	97.5 \pm 1.25	96.56 \pm 2 \pm 14.8	41.86 \pm 1.78	75.23 \pm 1.72	68.56 \pm 1.33	67.3 \pm 0.48	89.33 \pm 0.81	81.83 \pm 1.65	90.39 \pm 0.33	4.30
ACM-Snowball-2	95.08 \pm 3.11	96.38 \pm 2.59	95.74 \pm 2.22	41.4 \pm 1.23	68.51 \pm 1.7	55.97 \pm 2.03	OOM	88.83 \pm 1.49	81.58 \pm 1.23	90.81 \pm 0.52	7.44
ACM-Snowball-3	94.26 \pm 2.57	96.62 \pm 1.86	94.75 \pm 2.41	41.27 \pm 0.8	68.4 \pm 2.05	55.73 \pm 2.39	OOM	89.59 \pm 1.58	81.32 \pm 0.97	91.44 \pm 0.59	7.22
ACMII-GCN	95.9 \pm 1.83	96.62 \pm 2.44	95.08 \pm 2.07	41.84 \pm 1.15	68.38 \pm 1.36	54.53 \pm 2.09	67.15 \pm 0.41	89.00 \pm 0.72	81.79 \pm 0.95	90.74 \pm 0.5	5.90
ACMII-Snowball-2	95.25 \pm 1.55	96.63 \pm 2.24	95.25 \pm 1.55	41.1 \pm 0.75	67.83 \pm 2.63	53.48 \pm 0.6	OOM	88.95 \pm 1.04	82.07 \pm 1.04	90.56 \pm 0.39	7.56
ACMII-Snowball-3	93.61 \pm 2.79	97.00 \pm 2.63	94.75 \pm 3.09	40.31 \pm 1.6	67.53 \pm 2.83	52.31 \pm 1.57	OOM	89.36 \pm 1.26	81.56 \pm 1.15	91.31 \pm 0.6	9.00
ACMII-GCN+	93.93 \pm 3.03	96.75 \pm 1.79	95.41 \pm 2.82	41.5 \pm 1.54	75.51 \pm 1.58	69.81 \pm 1.11	67.44 \pm 0.31	89.18 \pm 1.11	81.87 \pm 1.38	90.96 \pm 0.62	4.4
ACMII-GCN++	92.62 \pm 2.57	97.13 \pm 1.68	94.75 \pm 2.91	41.66 \pm 1.42	75.93 \pm 1.71	69.98 \pm 1.53	67.5 \pm 0.53	89.47 \pm 1.08	81.76 \pm 1.25	90.63 \pm 0.56	5.10

Table 2: Experimental results: average test accuracy \pm standard deviation on 10 real-world benchmark datasets. The best results are highlighted in grey and the best baseline results (SOTA in Figure 6) are underlined. Results "*" are reported from [8, 26] and results "†" are from [35]. NA means the reported results are not available and OOM means out of memory.

¹⁶The splits for all these experiments are random 60%/20%/20% splits for train/valid/test. The open source code we use is from <https://github.com/jianhao2016/GPRGNN/blob/f4aaad6ca28c83d3121338a4c4fe5d162edfa9a2/src/utils.py#L16>. See table 3 in Appendix A.2 for the performance comparison with several SOTA models on the fixed 48%/32%/20% splits provided by [35].

A.2 Comparison with SOTA Models on Fixed 48%/32%/20% Splits

See table 3 for the results and table 13 14 the optimal searched hyperparameters. The results and comparison give us the same conclusion as in Appendix A.1.

Datasets/Models	Cornell	Wisconsin	Texas	Film	Chameleon	Squirrel	Cora	Citeseer	PubMed	Average Rank
Geom-GCN	60.54 \pm 3.67	64.51 \pm 3.66	66.76 \pm 2.72	31.59 \pm 1.15	60.00 \pm 2.81	38.15 \pm 0.92	85.35 \pm 1.57	78.02 \pm 1.15	89.95 \pm 0.47	18.22
H ₂ GCN	82.70 \pm 5.28	87.65 \pm 4.98	84.86 \pm 7.23	35.70 \pm 1.00	60.11 \pm 2.15	36.48 \pm 1.86	87.87 \pm 1.20	77.11 \pm 1.57	89.49 \pm 0.38	15.11
GPRGCN	78.11 \pm 6.55	82.55 \pm 6.23	81.35 \pm 5.32	35.16 \pm 0.9	62.59 \pm 2.04	46.31 \pm 2.46	87.95 \pm 1.18	77.13 \pm 1.67	87.54 \pm 0.38	17.67
FAGCN	76.76 \pm 5.87	79.61 \pm 1.58	76.49 \pm 2.87	34.82 \pm 1.35	46.07 \pm 2.11	30.83 \pm 0.69	88.05 \pm 1.57	77.07 \pm 2.05	88.09 \pm 1.38	20.00
GCNII	77.86 \pm 3.79	80.39 \pm 3.40	77.57 \pm 3.83	37.44 \pm 1.30	63.86 \pm 3.04	38.47 \pm 1.58	88.37 \pm 1.25	77.33 \pm 1.48	90.15 \pm 0.43	12.44
MixHop	73.51 \pm 6.34	75.88 \pm 4.90	77.84 \pm 7.73	32.22 \pm 2.34	60.50 \pm 2.53	43.80 \pm 1.48	87.61 \pm 0.85	76.26 \pm 1.33	85.31 \pm 0.61	20.78
WRGAT	81.62 \pm 3.90	86.98 \pm 3.78	83.62 \pm 5.50	36.53 \pm 0.77	65.24 \pm 0.87	48.85 \pm 0.78	88.20 \pm 2.26	76.81 \pm 1.89	88.52 \pm 0.92	14.33
GGCN	85.68 \pm 6.63	86.86 \pm 3.29	84.86 \pm 4.55	37.54 \pm 1.56	71.14 \pm 1.84	55.17 \pm 1.58	87.95 \pm 1.05	77.14 \pm 1.45	89.15 \pm 0.37	10.22
LINKX	77.84 \pm 5.81	75.49 \pm 5.72	74.60 \pm 8.37	36.10 \pm 1.55	68.42 \pm 1.38	61.81 \pm 1.80	84.64 \pm 1.13	73.19 \pm 0.99	87.86 \pm 0.77	18.78
GloGNN	83.51 \pm 4.26	87.06 \pm 3.53	84.32 \pm 4.15	37.35 \pm 1.30	69.78 \pm 2.42	57.54 \pm 1.39	88.31 \pm 1.13	77.41 \pm 1.65	89.62 \pm 0.35	8.78
GloGNN++	85.95 \pm 5.10	88.04 \pm 3.22	84.05 \pm 4.90	37.70 \pm 1.40	71.21 \pm 1.84	57.88 \pm 1.76	88.33 \pm 1.09	77.22 \pm 1.78	89.24 \pm 0.39	7.33
ACM-SGC-1	82.43 \pm 5.44	86.47 \pm 3.77	81.89 \pm 4.53	35.49 \pm 1.06	63.99 \pm 1.66	45.00 \pm 1.4	86.9 \pm 1.38	76.73 \pm 1.59	88.49 \pm 0.51	17.56
ACM-SGC-2	82.43 \pm 5.44	86.47 \pm 3.77	81.89 \pm 4.53	36.04 \pm 0.83	59.21 \pm 2.22	40.02 \pm 0.96	87.69 \pm 1.07	76.59 \pm 1.69	89.01 \pm 0.6	17.67
Diag-NSD	86.49 \pm 7.35	88.63 \pm 2.75	85.67 \pm 6.95	37.79 \pm 1.01	68.68 \pm 1.73	54.78 \pm 1.81	87.14 \pm 1.06	77.14 \pm 1.85	89.42 \pm 0.43	9.00
O(d)-NSD	84.86 \pm 4.71	89.41 \pm 4.74	85.95 \pm 5.51	37.81 \pm 1.15	68.04 \pm 1.58	56.34 \pm 1.32	86.90 \pm 1.13	76.70 \pm 1.57	89.49 \pm 0.40	10.44
Gen-NSD	85.68 \pm 6.51	89.21 \pm 3.84	82.97 \pm 5.13	37.80 \pm 1.22	67.93 \pm 1.58	53.17 \pm 1.31	87.30 \pm 1.15	76.32 \pm 1.65	89.33 \pm 0.35	11.67
NLMLP	84.9 \pm 5.7	87.3 \pm 4.3	85.4 \pm 3.8	37.9 \pm 1.3	50.7 \pm 2.2	33.7 \pm 1.5	76.9 \pm 1.8	73.4 \pm 1.9	88.2 \pm 0.5	16.67
NLGCN	57.6 \pm 5.5	60.2 \pm 5.3	65.5 \pm 6.6	31.6 \pm 1.0	70.1 \pm 2.9	59.0 \pm 1.2	88.1 \pm 1.0	75.2 \pm 1.4	89.0 \pm 0.5	17.44
NLGAT	54.7 \pm 7.6	56.9 \pm 7.3	62.6 \pm 7.1	29.5 \pm 1.3	65.7 \pm 1.4	56.8 \pm 2.5	88.5 \pm 1.8	76.2 \pm 1.6	88.2 \pm 0.3	18.56
ACM-GCN	85.14 \pm 6.07	88.43 \pm 3.22	87.84 \pm 4.4	36.63 \pm 0.84	69.14 \pm 1.91	55.19 \pm 1.49	87.91 \pm 0.95	77.32 \pm 1.7	90.00 \pm 0.52	8.11
ACMII-GCN	85.95 \pm 5.64	87.45 \pm 3.74	86.76 \pm 4.75	36.31 \pm 1.2	68.46 \pm 1.7	51.8 \pm 1.5	88.01 \pm 1.08	77.15 \pm 1.45	89.89 \pm 0.43	9.33
ACM-GCN+	85.68 \pm 4.84	88.43 \pm 2.39	88.38 \pm 3.64	36.26 \pm 1.34	74.47 \pm 1.84	66.98 \pm 1.71	88.05 \pm 0.99	77.67 \pm 1.19	89.82 \pm 0.41	5.33
ACMII-GCN+	85.41 \pm 5.3	88.04 \pm 3.66	88.11 \pm 3.24	36.14 \pm 1.44	74.56 \pm 2.08	67.07 \pm 1.65	88.19 \pm 1.17	77.2 \pm 1.61	89.78 \pm 0.49	6.78
ACM-GCN++	85.68 \pm 5.8	88.24 \pm 3.16	88.38 \pm 3.43	37.31 \pm 1.09	74.41 \pm 1.49	67.06 \pm 1.66	88.11 \pm 0.96	77.46 \pm 1.65	89.65 \pm 0.58	5.33
ACMII-GCN++	86.49 \pm 6.73	88.43 \pm 3.66	88.38 \pm 3.43	37.09 \pm 1.32	74.76 \pm 2.2	67.4 \pm 2.21	88.25 \pm 0.96	77.12 \pm 1.58	89.71 \pm 0.48	4.78

Table 3: Experimental results on fixed splits provided by [35]: average test accuracy \pm standard deviation on 9 real-world benchmark datasets. The best results are highlighted. Results of Geom-GCN, H₂GCN and GPRGCN, LINX, GloGNN, GloGNN++, Diag-NSD, O(d)-NSD, Gen-NSD, NLMLP, NLGCN and NLGAT are from [35, 45, 27, 26, 24, 5, 28]; results on the rest models are run by ourselves and the hyperparameter searching range is the same as table 9.

A.3 Discussion of Random Walk and Symmetric Renormalized Filters

Datasets/Models	RW		Symmetric	
	ACM	ACMII	ACM	ACMII
Cornell	94.75 \pm 3.8	95.9 \pm 1.83	94.92 \pm 2.48	94.1 \pm 2.56
Wisconsin	95.75 \pm 2.03	96.62 \pm 2.44	95.63 \pm 2.81	96.25 \pm 2.5
Texas	94.92 \pm 2.88	95.08 \pm 2.07	94.75 \pm 2.01	94.59 \pm 2.65
Film	41.62 \pm 1.15	41.84 \pm 1.15	41.58 \pm 1.3	41.65 \pm 0.6
Chameleon	69.04 \pm 1.74	68.38 \pm 1.36	67.9 \pm 2.76	68.03 \pm 1.68
Squirrel	58.02 \pm 1.86	54.53 \pm 2.09	54.18 \pm 1.35	53.68 \pm 1.74
Cora	88.62 \pm 1.22	89.00 \pm 0.72	88.65 \pm 1.26	88.19 \pm 1.38
Citeseer	81.68 \pm 0.97	81.79 \pm 0.95	81.84 \pm 1.15	81.81 \pm 0.86
PubMed	90.66 \pm 0.47	90.74 \pm 0.5	90.59 \pm 0.81	90.54 \pm 0.59

Table 4: Comparison of random walk and symmetric renormalized filters

The definitions of the similarity matrix, (modified) aggregation similarity score and diversification distinguishability value can be extended to symmetric normalized Laplacian or other aggregation operations. Yet unfortunately, we cannot extend Theorem 1 at this moment, because we need a condition that the row sum of \hat{A} is not greater than 1 in the proof. This condition is guaranteed for random walk normalized Laplacian but not for symmetric normalized Laplacian. While in practice, we evaluate our models with symmetric filters and compare them with random walk filters. From table 4 we can see that, there are no big differences between these two filters.

Datasets/Models	With W_{mix}		Without W_{mix}	
	ACM	ACMII	ACM	ACMII
Cornell	94.75 \pm 3.8	95.9 \pm 1.83	93.61 \pm 2.37	90.49 \pm 2.72
Wisconsin	95.75 \pm 2.03	96.62 \pm 2.44	95 \pm 2.5	97.50 \pm 1.25
Texas	94.92 \pm 2.88	95.08 \pm 2.07	94.92 \pm 2.79	94.92 \pm 2.79
Film	41.62 \pm 1.15	41.84 \pm 1.15	40.79 \pm 1.01	40.86 \pm 1.48
Chameleon	69.04 \pm 1.74	68.38 \pm 1.36	68.16 \pm 1.79	66.78 \pm 2.79
Squirrel	58.02 \pm 1.86	54.53 \pm 2.09	55.35 \pm 1.72	52.98 \pm 1.66
Cora	88.62 \pm 1.22	89.00 \pm 0.72	88.41 \pm 1.63	88.72 \pm 1.5
Citeseer	81.68 \pm 0.97	81.79 \pm 0.95	81.65 \pm 1.48	81.72 \pm 1.58
PubMed	90.66 \pm 0.47	90.74 \pm 0.5	90.46 \pm 0.69	90.39 \pm 1.33

Table 5: Ablation study of W_{mix}

A.4 Ablation Study of W_{mix}

From table 5 we can see that ACM(II) with W_{mix} shows superiority in most datasets, although it is not statistically significant on some of them.

One possible explanation of the function of W_{mix} is that it could help alleviate the dominance and bias to majority: Suppose in a dataset, most of the nodes need more information from LP channel than HP and identity channels, then W_L, W_H, W_I tend to learn larger α_L than α_H and α_I . For the minority nodes that need more information from HP or identity channels, they are hard to get large α_H or α_I values because W_L, W_H, W_I are biased to the majority. And W_{mix} can help us to learn more diverse alpha values when W_L, W_H, W_I are biased.

Attention with more complicated design can be found for the node-wise adaptive channel mixing mechanism, but we do not explore this direction deeper in this paper because investigating attention function is not the main contribution of our paper.

A.5 Learn Weights with Raw Features v.s. Combined Features

Datasets/Models	With Raw Features		With Combined Features	
	ACM	ACMII	ACM	ACMII
Cornell	94.75 \pm 3.8	95.9 \pm 1.83	95.08 \pm 2.64	93.93 \pm 3.52
Wisconsin	95.75 \pm 2.03	96.62 \pm 2.44	96.12 \pm 1.31	96 \pm 2
Texas	94.92 \pm 2.88	95.08 \pm 2.07	94.92 \pm 2.48	94.59 \pm 2.94
Film	41.62 \pm 1.15	41.84 \pm 1.15	41.62 \pm 1.34	41.44 \pm 1.18
Chameleon	69.04 \pm 1.74	68.38 \pm 1.36	68.82 \pm 2.18	68.53 \pm 3.08
Squirrel	58.02 \pm 1.86	54.53 \pm 2.09	57.48 \pm 1.68	53.28 \pm 1.08
Cora	88.62 \pm 1.22	89.00 \pm 0.72	88.59 \pm 1.04	88.75 \pm 0.83
Citeseer	81.68 \pm 0.97	81.79 \pm 0.95	81.9 \pm 1.27	81.76 \pm 1.05
PubMed	90.66 \pm 0.47	90.74 \pm 0.5	90.75 \pm 0.77	90.58 \pm 0.64

Table 6: Performance comparison between raw features and combined features

Construct the combined feature $H_{\text{Comb}}^l = [H_L^l, H_H^l, H_I^l]$, Replace the first line in Step 2 by the following lines:

$$\begin{aligned} \tilde{\alpha}_L^l &= \sigma(H_{\text{Comb}}^l \tilde{W}_L^l), \quad \tilde{\alpha}_H^l = \sigma(H_{\text{Comb}}^l \tilde{W}_H^l), \quad \tilde{\alpha}_I^l = \sigma(H_{\text{Comb}}^l \tilde{W}_I^l), \quad \tilde{W}_L^{l-1}, \tilde{W}_H^{l-1}, \tilde{W}_I^{l-1} \in \mathbb{R}^{3F_l \times 1} \\ [\tilde{\alpha}_L^l, \tilde{\alpha}_H^l, \tilde{\alpha}_I^l] &= \text{Softmax}(([\tilde{\alpha}_L^l, \tilde{\alpha}_H^l, \tilde{\alpha}_I^l] / T) W_{\text{Mix}}^l) \in \mathbb{R}^{N \times 3}, \quad T \in \mathbb{R} \text{ temperature}, \quad W_{\text{Mix}}^l \in \mathbb{R}^{3 \times 3}; \end{aligned}$$

The performance comparison can be found in table 6. From the results, we do not find significant difference between the frameworks with combined features and raw features. The reason is that the necessary nonlinear information from each channel is combined in $[\tilde{\alpha}_L^l, \tilde{\alpha}_H^l, \tilde{\alpha}_I^l]$ and W_{Mix}^l is enough

to learn to mix the combined weights from different channels. The learning of redundant information in the feature extraction step for each channel will not improve the performance. Meanwhile, A disadvantage of the combined feature is that it increases the computational cost. Thus, we decide to use the raw features.

A.6 H_{node}^v Distributions of Different Datasets

See Figure 7 for H_{node}^v distributions. We can see that *Wisconsin* and *Texas* have high density in low homophily area, *Cornell*, *Chameleon*, *Squirrel* and *Film* have high density in low and middle homophily area, *Cora*, *CiteSeer* and *PubMed* have high density in high homophily area.

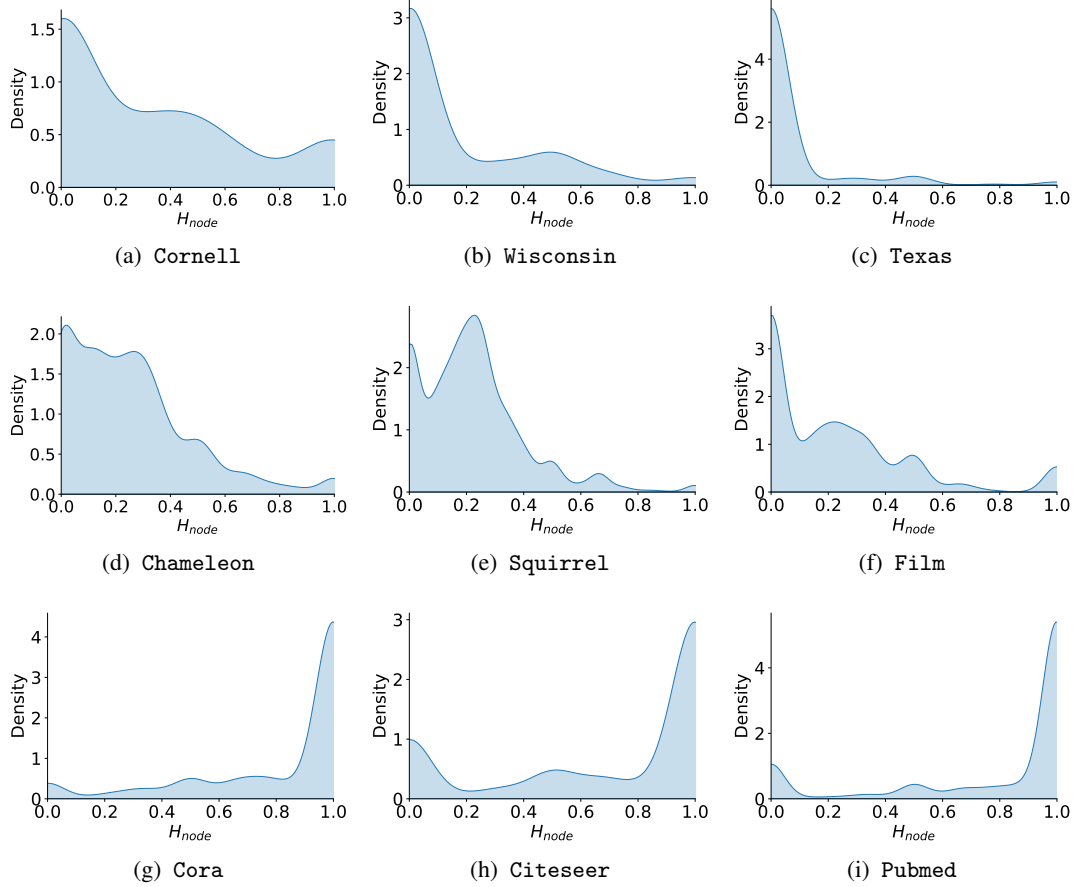


Figure 7: H_{node}^v distributions of different datasets

A.7 Distributions of Learned $\alpha_L, \alpha_H, \alpha_I$ in the Hidden and Output Layers of ACN-GCN

See Figure 8 for the distributions of weights in hidden layers and Figure 9 for the distributions of weights in output layers.

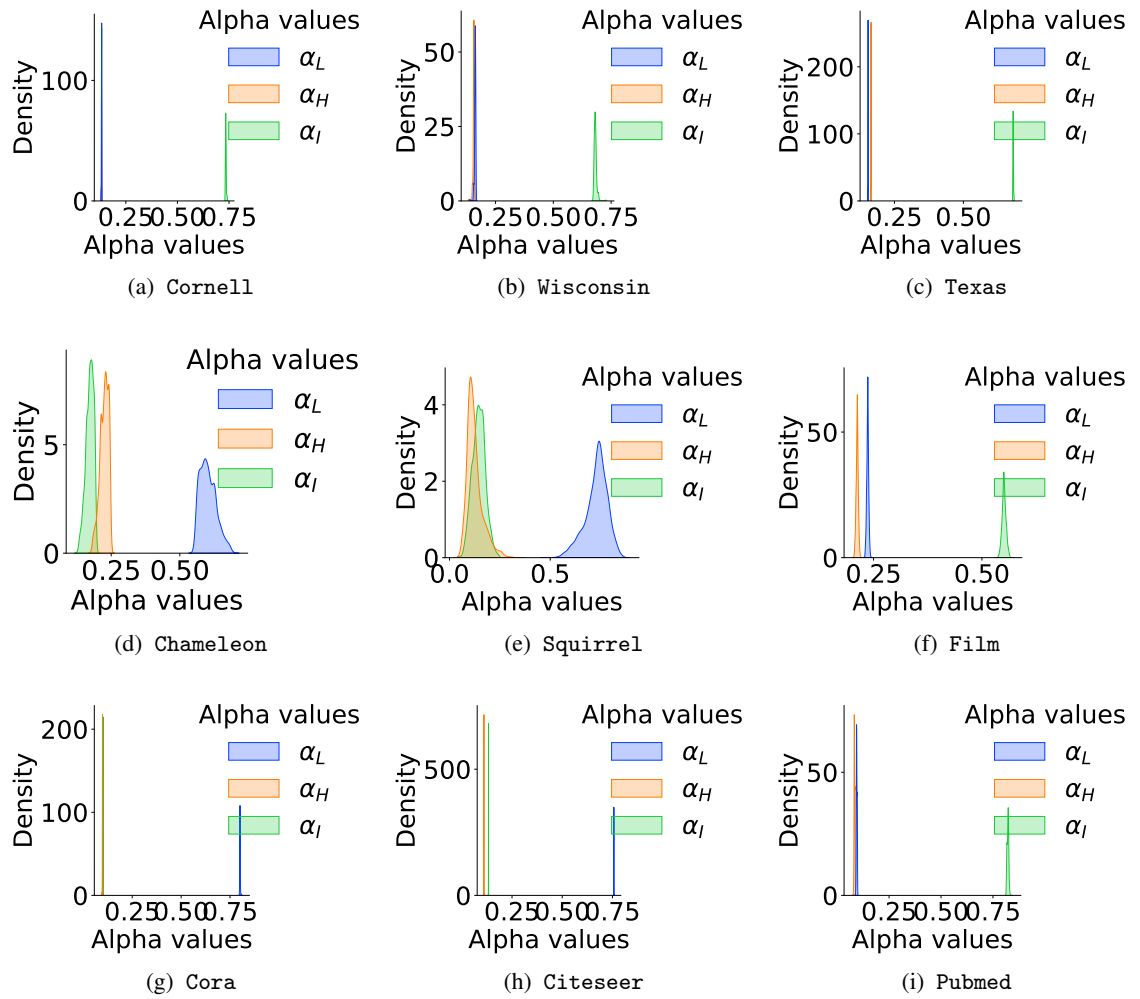


Figure 8: Distributions of the learned $\alpha_L, \alpha_H, \alpha_I$ in the hidden layer of ACM-GCN

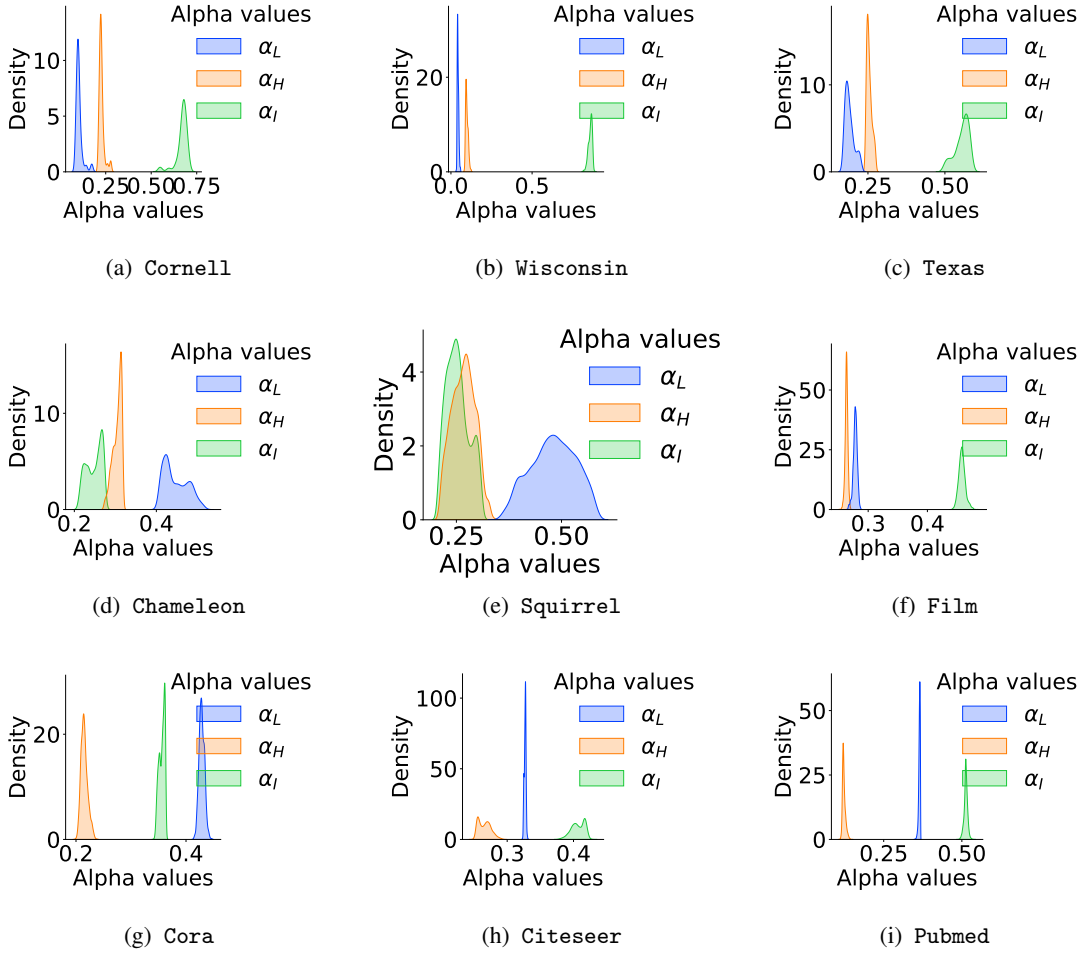


Figure 9: Distributions of the learned $\alpha_L, \alpha_H, \alpha_I$ in the output layer of ACM-GCN

B Details of the Implementation

B.1 Implementation of ACM-GCMII

Unlike other baseline GNN models, GCNII and GCNII* are not able to be applied under ACMII framework and we will make an explanation as follows.

$$\begin{aligned} \text{GCNII: } \mathbf{H}^{(\ell+1)} &= \sigma \left(\left((1 - \alpha_\ell) \hat{\mathbf{A}} \mathbf{H}^{(\ell)} + \alpha_\ell \mathbf{H}^{(0)} \right) \left((1 - \beta_\ell) \mathbf{I}_n + \beta_\ell \mathbf{W}^{(\ell)} \right) \right) \\ \text{GCNII*: } \mathbf{H}^{(\ell+1)} &= \sigma \left((1 - \alpha_\ell) \hat{\mathbf{A}} \mathbf{H}^{(\ell)} \left((1 - \beta_\ell) \mathbf{I}_n + \beta_\ell \mathbf{W}_1^{(\ell)} \right) + \alpha_\ell \mathbf{H}^{(0)} \left((1 - \beta_\ell) \mathbf{I}_n + \beta_\ell \mathbf{W}_2^{(\ell)} \right) \right) \end{aligned}$$

From the above formulas of GCNII and GCNII* we can see that, without major modification, GCNII and GCNII* are hard to be put into ACMII framework. In ACMII framework, before apply $\hat{\mathbf{A}}$, we first implement a nonlinear feature extractor $\sigma(H^\ell \mathbf{W}^{(\ell)})$. But in GCNII and GCNII*, before multiplying W^ℓ (or W_1^ℓ, W_2^ℓ) to extract features, we need to add another term including $H^{(0)}$, which are not filtered by $\hat{\mathbf{A}}$. This makes the order of aggregator $\hat{\mathbf{A}}$ and nonlinear extractor unexchangeable and thus, incompatible with ACMII framework. So we did not implement GCNII and GCNII* in ACMII framework.

B.2 Implementation of ACM(II)-GCN+ and ACM(II)-GCN++

Besides the features extracted by different filters, some recent SOTA models use additional graph structure information explicitly, *i.e.*, $\text{MLP}_\theta(A)$, to address heterophily problem, *e.g.*, LINKX [25] and GloGNN [24] and is found effective on some datasets, *e.g.*, *Chameleon*, *Squirrel*. The explicit structure information can be directly incorporated into ACM and ACMII framework, and we have ACM(II)-GCN+ and ACM(II)-GCN++ as follows.

- ACM-GCN+ and ACMII-GCN+ have an option to include structure information channel (the 4-th channel) in each layer and their differences from ACM-GCN and ACMII-GCN are **highlighted in red** as follows,

Step 1. Feature Extraction for LP, HP, Identity and Structure Information Channel:

$$H_A^l = \text{ReLU}(AW_A^l), W_A^l \in \mathbb{R}^{N \times F_l}, \text{ get } H_L^l, H_H^l, H_I^l \text{ with the same step as ACM-GCN and ACMII-GCN.}$$

Step 2. Row-wise Feature-based Weight Learning with Layer Normalization (LN)

$$\tilde{H}_L^l = \text{LN}(H_L^l), \tilde{H}_H^l = \text{LN}(H_H^l), \tilde{H}_I^l = \text{LN}(H_I^l), \tilde{H}_A^l = \text{LN}(H_A^l),$$

$$\tilde{\alpha}_L^l = \text{Sigmoid}(\tilde{H}_L^l \tilde{W}_L^l), \tilde{\alpha}_H^l = \text{Sigmoid}(\tilde{H}_H^l \tilde{W}_H^l), \tilde{\alpha}_I^l = \text{Sigmoid}(\tilde{H}_I^l \tilde{W}_I^l), \tilde{\alpha}_A^l = \text{Sigmoid}(\tilde{H}_A^l \tilde{W}_A^l),$$

$$\tilde{W}_L^{l-1}, \tilde{W}_H^{l-1}, \tilde{W}_I^{l-1}, \tilde{W}_A^l \in \mathbb{R}^{F_l \times 1}$$

Step 3. Node-wise Adaptive Channel Mixing:

Option 1: without structure information

$$[\alpha_L^l, \alpha_H^l, \alpha_I^l] = \text{Softmax}(([[\tilde{\alpha}_L^l, \tilde{\alpha}_H^l, \tilde{\alpha}_I^l] / T] W_{\text{Mix}}^l) \in \mathbb{R}^{N \times 3}, T = 3 \text{ temperature}, W_{\text{Mix}}^l \in \mathbb{R}^{3 \times 3};$$

$$H^l = \text{ReLU}(\text{diag}(\alpha_L^l)H_L^l + \text{diag}(\alpha_H^l)H_H^l + \text{diag}(\alpha_I^l)H_I^l)$$

Option 2: with structure information

$$[\alpha_L^l, \alpha_H^l, \alpha_I^l, \alpha_A^l] = \text{Softmax}(([[\tilde{\alpha}_L^l, \tilde{\alpha}_H^l, \tilde{\alpha}_I^l, \tilde{\alpha}_A^l] / T] W_{\text{Mix}}^l) \in \mathbb{R}^{N \times 4}, T = 4 \text{ temperature}, W_{\text{Mix}}^l \in \mathbb{R}^{4 \times 4};$$

$$H^l = \text{ReLU}(\text{diag}(\alpha_L^l)H_L^l + \text{diag}(\alpha_H^l)H_H^l + \text{diag}(\alpha_I^l)H_I^l + \text{diag}(\alpha_A^l)H_A^l)$$

- ACM-GCN++ and ACMII-GCN++ have an option to include structure information channel (the 4-th channel) in each layer and residual connection and their differences from ACM-GCN+ and ACMII-GCN+ are **highlighted in red** as follows,

Step 1. Feature Extraction for LP, HP, Identity and Structure Information Channel, Get H_X :

$$H_X = \text{ReLU}(XW_X) \in \mathbb{R}^{F \times F'}, H_A^l = \text{ReLU}(AW_A^l), W_A^l \in \mathbb{R}^{N \times F'},$$

get H_L^l, H_H^l, H_I^l with the same step as ACM-GCN and ACMII-GCN.

Step 2. Row-wise Feature-based Weight Learning with Layer Normalization (LN)

$$\tilde{H}_L^l = \text{LN}(H_L^l), \tilde{H}_H^l = \text{LN}(H_H^l), \tilde{H}_I^l = \text{LN}(H_I^l), \tilde{H}_A^l = \text{LN}(H_A^l),$$

$$\tilde{\alpha}_L^l = \text{Sigmoid}(\tilde{H}_L^l \tilde{W}_L^l), \tilde{\alpha}_H^l = \text{Sigmoid}(\tilde{H}_H^l \tilde{W}_H^l), \tilde{\alpha}_I^l = \text{Sigmoid}(\tilde{H}_I^l \tilde{W}_I^l), \tilde{\alpha}_A^l = \text{Sigmoid}(\tilde{H}_A^l \tilde{W}_A^l),$$

$$\tilde{W}_L^{l-1}, \tilde{W}_H^{l-1}, \tilde{W}_I^{l-1}, \tilde{W}_A^l \in \mathbb{R}^{F' \times 1}$$

Step 3. Node-wise Adaptive Channel Mixing:

Option 1: without structure information

$$[\alpha_L^l, \alpha_H^l, \alpha_I^l] = \text{Softmax}(([[\tilde{\alpha}_L^l, \tilde{\alpha}_H^l, \tilde{\alpha}_I^l] / T] W_{\text{Mix}}^l) \in \mathbb{R}^{N \times 3}, T = 3 \text{ temperature}, W_{\text{Mix}}^l \in \mathbb{R}^{3 \times 3};$$

$$H^l = \text{ReLU}(\text{diag}(\alpha_L^l)H_L^l + \text{diag}(\alpha_H^l)H_H^l + \text{diag}(\alpha_I^l)H_I^l) + H_X$$

Option 2: with structure information

$$[\alpha_L^l, \alpha_H^l, \alpha_I^l, \alpha_A^l] = \text{Softmax}(([[\tilde{\alpha}_L^l, \tilde{\alpha}_H^l, \tilde{\alpha}_I^l, \tilde{\alpha}_A^l] / T] W_{\text{Mix}}^l) \in \mathbb{R}^{N \times 4}, T = 4 \text{ temperature}, W_{\text{Mix}}^l \in \mathbb{R}^{4 \times 4};$$

$$H^l = \text{ReLU}(\text{diag}(\alpha_L^l)H_L^l + \text{diag}(\alpha_H^l)H_H^l + \text{diag}(\alpha_I^l)H_I^l + \text{diag}(\alpha_A^l)H_A^l) + H_X$$

The results of ACM-GCN+, ACMII-GCN+, ACM-GCN++ and ACMII-GCN++ trained on random 60%/20%/20% splits are reported in table 2 in Appendix A.1. The results on fixed 48%/32%/20% splits are reported in table 3 in Appendix A.2.

Computing Resources For all experiments on synthetic datasets and real-world datasets, we use NVIDIA V100 GPUs with 16/32GB GPU memory, 8-core CPU, 16G Memory. The software implementation is based on PyTorch and PyTorch Geometric [12].

C Hyperparameter Searching Range & Optimal Hyperparameters

C.1 Hyperparameter Searching Range for Synthetic Experiments

Hyperparameter Searching Range for Synthetic Experiments					
Models\Hyperparameters	lr	weight_decay	dropout	hidden	
MLP-1	0.05	{5e-5, 1e-4, 5e-4, 1e-3, 5e-3}	-	-	
SGC-1	0.05	{5e-5, 1e-4, 5e-4, 1e-3, 5e-3}	-	-	
ACM-SGC-1	0.05	{5e-5, 1e-4, 5e-4, 1e-3, 5e-3}	{ 0.1, 0.3, 0.5, 0.7, 0.9}	-	
MLP-2	0.05	{5e-5, 1e-4, 5e-4, 1e-3, 5e-3}	{ 0.1, 0.3, 0.5, 0.7, 0.9}	64	
GCN	0.05	{5e-5, 1e-4, 5e-4, 1e-3, 5e-3}	{ 0.1, 0.3, 0.5, 0.7, 0.9}	64	
ACM-GCN	0.05	{5e-5, 1e-4, 5e-4, 1e-3, 5e-3}	{ 0.1, 0.3, 0.5, 0.7, 0.9}	64	

Table 7: Hyperparameter searching range for synthetic experiments

C.2 Hyperparameter Searching Range for Ablation Study

Hyperparameter Searching Range for Ablation Study					
Models\Hyperparameters	lr	weight_decay	dropout	hidden	
SGC-LP+HP	{0.01, 0.05, 0.1}	{0, 5e-6, 1e-5, 5e-5, 1e-4, 5e-4, 1e-3, 5e-3, 1e-2}	-	-	
SGC-LP+Identity	{0.01, 0.05, 0.1}	{0, 5e-6, 1e-5, 5e-5, 1e-4, 5e-4, 1e-3, 5e-3, 1e-2}	-	-	
ACM-SGC-no adaptive mixing	{0.01, 0.05, 0.1}	{0, 5e-6, 1e-5, 5e-5, 1e-4, 5e-4, 1e-3, 5e-3, 1e-2}	{0, 0.1, 0.2, 0.3, 0.4, 0.5, 0.6, 0.7, 0.8, 0.9}	-	
GCN-LP+HP	{0.01, 0.05, 0.1}	{0, 5e-6, 1e-5, 5e-5, 1e-4, 5e-4, 1e-3, 5e-3, 1e-2}	{0, 0.1, 0.2, 0.3, 0.4, 0.5, 0.6, 0.7, 0.8, 0.9}	64	
GCN-LP+Identity	{0.01, 0.05, 0.1}	{0, 5e-6, 1e-5, 5e-5, 1e-4, 5e-4, 1e-3, 5e-3, 1e-2}	{0, 0.1, 0.2, 0.3, 0.4, 0.5, 0.6, 0.7, 0.8, 0.9}	64	
ACM-GCN-no adaptive mixing	{0.01, 0.05, 0.1}	{0, 5e-6, 1e-5, 5e-5, 1e-4, 5e-4, 1e-3, 5e-3, 1e-2}	{0, 0.1, 0.2, 0.3, 0.4, 0.5, 0.6, 0.7, 0.8, 0.9}	64	

Table 8: Hyperparameter searching range for ablation study

C.3 Hyperparameter Searching Range for GNNs on Real-world Datasets

See table 9 for the hyperparameter searching range of baseline GNNs, ACM-GNNs, ACMII-GNNs and several SOTA models.

C.4 Searched Optimal Hyperparameters for Baselines and ACM(II)-GNNs on Real-world Tasks

See the reported optimal hyperparameters on random 60%/20%/20% splits for baseline GNNs in table 10, for ACM-GNNs and ACMII-GNNs in table 11 and for ACM(II)-GCN+ and ACM(II)-GCN++ in table 12.

See the reported optimal hyperparameters on fixed 48%/32%/20% splits for ACM(II)-GNNs and FAGCN in table 13 and for ACM(II)-GCN+ and ACM(II)-GCN++ in table 14.

Models	Hyperparameters	lr	weight_decay	dropout	hidden	lambda	alpha_l	head	layers	JK type
H2GCN		0.01	0.001	{0, 0.5}	{8, 16, 32, 64}	-	-	-	{1, 2}	-
MixHop		0.01	0.001	0.5	{8, 16, 32}	-	-	-	{2, 3}	-
GCN+JK		{0.1, 0.01, 0.001}	0.001	0.5	{4, 8, 16, 32, 64}	-	-	-	2	{max, cat}
GAT+JK		{0.1, 0.01, 0.001}	0.001	0.5	{4, 8, 12, 32}	-	-	{2,4,8}	2	{max, cat}
GCNII, GCNII*		0.01	{0, 5e-6, 1e-5, 5e-5, 1e-4, 5e-4, 1e-3} for Deezer-Europe and {0, 5e-6, 1e-5, 5e-5, 1e-4, 5e-4, 1e-3, 5e-3, 1e-2} for others	0.5	64	{0.5, 1, 1.5}	{0.1,0.2,0.3,0.4,0.5}	{4, 8, 16, 32} for Deezer-Europe and {4, 8, 16, 32, 64} for others	{4, 8, 16, 32}	-
Baselines: {SGC-1, SGC-2, GCN, Snowball-2, Snowball-3, FAGCN}; ACM-{SGC-1, SGC-2, GCN, GCN+, GCN++, Snowball-2, Snowball-3}; ACMII-{SGC-1, SGC-2, GCN, GCN+, GCN++, Snowball-2, Snowball-3}		{0.002, 0.01, 0.05} for Europe and {0.01, 0.05, 0.1} for others	{0, 5e-6, 1e-5, 5e-5, 1e-4, 5e-4, 1e-3} for Deezer-Europe and {0, 5e-6, 1e-5, 5e-5, 1e-4, 5e-4, 1e-3, 5e-3, 1e-2} for others	{0, 0.1, 0.2, 0.3, 0.4, 0.5, 0.6, 0.7, 0.8, 0.9}	64	-	-	-	-	-
GraphSAGE		{0.01,0.05, 0.1}	{0, 5e-6, 1e-5, 5e-5, 1e-4, 5e-4, 1e-3} for Deezer-Europe and {0, 5e-6, 1e-5, 5e-5, 1e-4, 5e-4, 1e-3, 5e-3, 1e-2} for others	{ 0, 0.1, 0.2, 0.3, 0.4, 0.5, 0.6, 0.7, 0.8, 0.9}	8 for Deezer-Europe and 64 for others	-	-	-	-	-
ACM-{GCNII, GCNII*}		0.01	{0, 5e-6, 1e-5, 5e-5, 1e-4, 5e-4, 1e-3} for Deezer-Europe and {0, 5e-6, 1e-5, 5e-5, 1e-4, 5e-4, 1e-3, 5e-3, 1e-2} for others	{ 0, 0.1, 0.2, 0.3, 0.4, 0.5, 0.6, 0.7, 0.8, 0.9}	64	-	-	-	{1,2,3,4}	-

Table 9: Hyperparameter searching range for training on real-world datasets

Hyperparameters for Baseline GNNs																	
Datasets	Model\Hyperparameters	lr	weight_decay	dropout	hidden	# layers	Gat heads	JK Type	lambda	alpha_1	results	std	average epoch time/average total time				
Cornell	SGC-1	0.05	1.00e-02	0	64	-	-	-	-	-	70.98	8.39	2.53ms/0.51s				
	SGC-2	0.05	1.00e-03	0	64	-	-	-	-	-	72.62	9.92	2.46ms/0.53s				
	GCN	0.1	5.00e-03	0.5	64	2	-	-	-	-	82.46	3.11	3.67ms/0.74s				
	Snowball-2	0.01	5.00e-03	0.4	64	2	-	-	-	-	82.62	2.34	4.24ms/0.87s				
	Snowball-3	0.01	5.00e-03	0.4	64	3	-	-	-	-	82.95	2.1	6.66ms/1.36s				
	GCNII	0.01	1.00e-03	0.5	64	16	-	-	0.5	0.5	89.18	3.96	25.41ms/8.11s				
	GCNII*	0.01	1.00e-03	0.5	64	8	-	-	0.5	0.5	90.49	4.45	15.35ms/4.05s				
	FAGCN	0.01	1.00e-04	0.7	32	2	-	-	-	-	88.03	5.6	8.1ms/3.8858s				
	Mixhop	0.01	0.001	0.5	16	2	-	-	-	-	60.33	28.53	10.379ms/2.105s				
	H2GCN	0.01	0.001	0.5	64	1	-	-	-	-	86.23	4.71	4.381ms/1.123s				
Wisconsin	GCN+JK	0.1	0.001	0.5	64	2	-	cat	-	-	66.56	13.82	5.589ms/1.227s				
	GAT+JK	0.1	0.001	0.5	32	2	8	max	-	-	74.43	10.24	10.725ms/2.478s				
	SGC-1	0.05	5.00e-03	0	64	-	-	-	-	-	70.38	2.85	2.83ms/0.57s				
	SGC-2	0.1	1.00e-03	0	64	-	-	-	-	-	74.75	2.89	2.14ms/0.43s				
	GCN	0.1	1.00e-03	0.7	64	2	-	-	-	-	75.5	2.92	3.74ms/0.76s				
	Snowball-2	0.1	1.00e-03	0.5	64	2	-	-	-	-	74.88	3.42	3.73ms/0.76s				
	Snowball-3	0.05	5.00e-04	0.8	64	3	-	-	-	-	69.5	5.01	5.46ms/1.12s				
	GCNII	0.01	1.00e-03	0.5	64	8	-	-	0.5	0.5	83.25	2.69					
	GCNII*	0.01	1.00e-03	0.5	64	4	-	-	1.5	0.3	89.12	3.06	9.26ms/1.96s				
	FAGCN	0.05	1.00e-04	0	32	2	-	-	-	-	89.75	6.37	12.9ms/4.6359s				
Texas	Mixhop	0.01	0.001	0.5	16	2	-	-	-	-	77.25	7.80	10.281ms/2.095s				
	H2GCN	0.01	0.001	0.5	32	1	-	-	-	-	87.5	1.77	4.324ms/1.134s				
	GCN+JK	0.1	0.001	0.5	32	2	-	cat	-	-	62.5	15.75	5.117ms/1.049s				
	GAT+JK	0.1	0.001	0.5	4	2	8	max	-	-	69.5	3.12	10.762ms/2.25s				
	APPNP	0.05	0.001	0.5	64	2	-	-	-	-	92	3.59	10.303ms/2.104s				
	GPRGNN	0.05	0.001	0.5	256	2	-	-	-	-	93.75	2.37	11.856ms/2.415s				
	SGC-1	0.05	1.00e-03	0	64	-	-	-	-	-	83.28	5.43	2.55ms/0.54s				
	SGC-2	0.01	1.00e-03	0	64	-	-	-	-	-	81.31	3.3	2.61ms/0.53s				
	GCN	0.05	1.00e-02	0.9	64	2	-	-	-	-	83.11	3.2	3.59ms/0.73s				
	Snowball-2	0.05	1.00e-02	0.9	64	2	-	-	-	-	83.11	3.2	3.98ms/0.82s				
Film	Snowball-3	0.05	1.00e-02	0.9	64	3	-	-	-	-	83.11	3.2	5.56ms/1.12s				
	GCNII	0.01	1.00e-04	0.5	64	4	-	-	1.5	0.5	82.46	4.58					
	GCNII*	0.01	1.00e-04	0.5	64	8	-	-	0.5	0.5	88.52	3.02	15.64ms/3.47s				
	FAGCN	0.01	5.00e-04	0	32	2	-	-	-	-	88.85	4.39	8.8ms/6.5252s				
	Mixhop	0.01	0.001	0.5	32	2	-	-	-	-	76.39	7.66	11.090ms/2.329s				
	H2GCN	0.01	0.001	0.5	64	1	-	-	-	-	85.90	3.53	4.197ms/0.95s				
	GCN+JK	0.1	0.001	0.5	32	2	-	cat	-	-	80.66	1.91	5.28ms/1.085s				
	GAT+JK	0.1	0.001	0.5	8	2	2	cat	-	-	75.41	7.18	10.937ms/2.402s				
	SGC-1	0.01	5.00e-06	0	64	-	-	-	-	-	25.26	1.18	3.18ms/0.70s				
	SGC-2	0.01	5.00e-06	0	64	-	-	-	-	-	28.81	1.11	2.13ms/0.43s				
Chameleon	GCN	0.1	5.00e-04	0	64	2	-	-	-	-	35.51	0.99	4.86ms/0.99s				
	Snowball-2	0.1	5.00e-04	0	64	2	-	-	-	-	35.97	0.66	5.59ms/1.14s				
	Snowball-3	0.1	5.00e-04	0.2	64	3	-	-	-	-	36	1.36	7.89ms/1.60s				
	GCNII	0.01	1.00e-04	0.5	64	8	-	-	1.5	0.3	40.82	1.79	15.85ms/3.22s				
	GCNII*	0.01	1.00e-06	0.5	64	4	-	-	1	0.1	41.54	0.99	45.4ms/11.107s				
	FAGCN	0.01	5.00e-05	0.6	32	2	-	-	-	-	31.59	1.37	17.651ms/3.566s				
	Mixhop	0.01	0.001	0.5	16	2	8	max	-	-	33.13	2.40	17.651ms/3.566s				
	H2GCN	0.01	0.001	0	32	1	8	max	-	-	38.85	1.17	8.101ms/1.695s				
	GCN+JK	0.1	0.001	0.5	32	2	8	cat	-	-	32.72	2.62	8.946ms/1.807s				
	GAT+JK	0.001	0.001	0.5	4	2	8	cat	-	-	35.41	0.97	20.726ms/4.187s				
Squirrel	SGC-1	0.1	5.00e-06	0	64	-	-	-	-	-	64.86	1.81	3.48ms/2.96s				
	SGC-2	0.1	0.00e+00	0	64	-	-	-	-	-	62.67	2.41	4.43ms/1.12s				
	GCN	0.01	1.00e-05	0.9	64	2	-	-	-	-	64.18	2.62	4.96ms/1.18s				
	Snowball-2	1.00e-01	1.00e-05	0.9	64	2	-	-	-	-	64.99	2.39	4.96ms/1.00s				
	Snowball-3	0.1	5.00e-06	0.9	64	3	-	-	-	-	65.49	1.64	7.44ms/1.50s				
	GCNII	0.01	5.00e-06	0.5	64	4	-	-	0.5	0.1	60.35	2.7	9.76ms/2.26s				
	GCNII*	0.01	5.00e-04	0.5	64	4	-	-	1.5	0.5	62.8	2.87	10.40ms/2.17s				
	FAGCN	0.002	1.00e-04	0	32	2	-	-	-	-	49.47	2.84	8.4ms/13.8696s				
	Mixhop	0.01	0.001	0.5	16	2	8	max	-	-	36.28	10.2	11.372ms/2.297s				
	H2GCN	0.01	0.001	0	32	1	8	max	-	-	52.3	0.48	4.059ms/0.82s				
Cora	GCN+JK	0.001	0.001	0.5	32	2	8	cat	-	-	64.68	2.85	5.211ms/1.053s				
	GAT+JK	0.001	0.001	0.5	4	2	8	max	-	-	68.14	1.18	13.772ms/2.788s				
	SGC-1	0.05	0.00e+00	0	64	-	-	-	-	-	47.62	1.27	4.65ms/1.44s				
	SGC-2	0.1	0.00e+00	0.9	64	-	-	-	-	-	41.25	1.4	35.00ms/7.81s				
	GCN	0.01	5.00e-05	0.7	64	2	-	-	-	-	44.76	1.39	8.41ms/2.50s				
	Snowball-2	0.1	0.00e+00	0.9	64	2	-	-	-	-	47.88	1.23	8.96ms/1.92s				
	Snowball-3	0.1	0.00e+00	0.8	64	3	-	-	-	-	48.25	0.94	14.00ms/2.90s				
	GCNII	0.01	1.00e-04	0.5	64	16	-	-	1.5	0.2	38.81	1.97	13.35ms/2.70s				
	GCNII*	0.01	5.00e-05	0.5	64	4	-	-	1.5	0.3	38.31	1.3	13.81ms/2.78s				
	FAGCN	0.05	1.00e-04	0	32	2	-	-	-	-	42.24	1.2	16ms/6.7961s				
CiteSeer	Mixhop	0.01	0.001	0.5	32	2	-	-	-	-	24.55	2.6	17.634ms/3.562s				
	H2GCN	0.01	0.001	0	16	1	-	-	-	-	30.39	1.22	9.315ms/1.882s				
	GCN+JK	0.001	0.001	0.5	32	2	-	max	-	-	53.4	1.9	14.321ms/2.905s				
	GAT+JK	0.001	0.001	0.5	8	2	4	max	-	-	52.28	3.61	29.097ms/5.878s				
	SGC-1	0.1	5.00e-04	0	64	-	-	-	-	-	79.66	0.75	3.43ms/7.30s				
	SGC-2	0.01	5.00e-04	0.9	64	-	-	-	-	-	80.75	1.15	5.33ms/4.40s				
	GCN	0.1	1.00e-03	0.9	64	2	-	-	-	-	81.39	1.23	4.18ms/0.86s				
	Snowball-2	0.1	1.00e-03	0.8	64	2	-	-	-	-	81.53	1.71	5.19ms/1.11s				
	Snowball-3	0.1	1.00e-03	0.9	64	3	-	-	-	-	80.93	1.32	7.64ms/1.69s				
PubMed	GCNII	0.01	1.00e-03	0.5	64	16	-										

Hyperparameters for ACM-GNNs and ACMII-GNNs														
Datasets	Models	Hyperparameters	lr	weight_decay	dropout	hidden	# layers	Gat heads	JK Type	lambda	alpha_1	results	std	average epoch time/average total time
Cornell	ACM-SGC-1	0.01	5.00E-03	0.6	64	-	-	-	-	-	-	93.77	1.91	5.53ms/2.31s
	ACM-SGC-2	0.01	5.00E-03	0.6	64	-	-	-	-	-	-	93.77	2.17	4.73ms/1.87s
	ACM-GCN	0.05	1.00E-02	0.2	64	2	-	-	-	-	-	94.75	3.8	8.25ms/1.69s
	ACMII-GCN	0.1	1.00E-02	0.5	64	2	-	-	-	-	-	95.25	2.79	8.43ms/1.71s
	ACM-GCNII	0.01	1.00E-03	0.5	64	1	-	-	-	0.5	0.4	92.62	3.13	6.81ms/1.43s
	ACM-GCNII*	0.01	5.00E-04	0.5	64	1	-	-	-	0.5	0.1	93.44	2.74	6.76ms/1.39s
	ACM-Snowball-2	0.05	1.00E-02	0.2	64	2	-	-	-	-	-	95.08	3.11	9.15ms/1.86s
	ACM-Snowball-3	0.1	1.00E-02	0.4	64	3	-	-	-	-	-	94.26	2.57	13.20ms/2.68s
	ACMII-Snowball-2	0.05	1.00E-02	0.6	64	2	-	-	-	-	-	95.25	1.55	8.23ms/1.72s
	ACMII-Snowball-3	0.05	1.00E-02	0.7	64	3	-	-	-	-	-	93.61	2.79	11.70ms/2.37s
Wisconsin	ACM-SGC-1	0.05	5.00E-03	0.7	64	-	-	-	-	-	-	93.25	2.92	5.96ms/1.34s
	ACM-SGC-2	0.1	5.00E-03	0.2	64	-	-	-	-	-	-	94	2.61	4.60ms/0.95s
	ACM-GCN	0.1	5.00E-03	0	64	2	-	-	-	-	-	95.75	2.03	8.11ms/1.64s
	ACMII-GCN	0.1	1.00E-02	0.2	64	2	-	-	-	-	-	96.62	2.44	8.28ms/1.68s
	ACM-GCNII	0.01	5.00E-03	0.5	64	1	-	-	-	1	0.1	94.63	2.96	9.31ms/2.19s
	ACM-GCNII*	0.01	1.00E-03	0.5	64	1	-	-	-	1.5	0.4	94.37	2.81	7.11ms/1.45s
	ACM-Snowball-2	0.1	5.00E-03	0.1	64	2	-	-	-	-	-	96.38	2.59	8.63ms/1.74s
	ACM-Snowball-3	0.05	1.00E-02	0.3	64	3	-	-	-	-	-	96.62	1.86	12.79ms/2.58s
	ACMII-Snowball-2	0.1	1.00E-02	0.1	64	2	-	-	-	-	-	96.63	2.24	8.11ms/1.65s
	ACMII-Snowball-3	0.1	5.00E-03	0.1	64	3	-	-	-	-	-	97	2.63	12.38ms/2.51s
Texas	ACM-SGC-1	0.01	5.00E-03	0.6	64	-	-	-	-	-	-	93.61	1.55	5.43ms/2.18s
	ACM-SGC-2	0.05	5.00E-03	0.4	64	-	-	-	-	-	-	93.44	2.54	4.59ms/1.01s
	ACM-GCN	0.05	1.00E-02	0.6	64	2	-	-	-	-	-	94.92	2.88	8.33ms/1.70s
	ACMII-GCN	0.1	5.00E-03	0.4	64	2	-	-	-	-	-	95.08	2.54	8.49ms/1.72s
	ACM-GCNII	0.01	1.00E-03	0.5	64	1	-	-	-	0.5	0.4	92.46	1.97	6.47ms/1.36s
	ACM-GCNII*	0.01	1.00E-03	0.5	64	1	-	-	-	0.5	0.4	93.28	2.79	7.03ms/1.45s
	ACM-Snowball-2	0.05	1.00E-02	0.1	64	2	-	-	-	-	-	95.74	2.22	8.35ms/1.71s
	ACM-Snowball-3	0.01	5.00E-03	0.6	64	3	-	-	-	-	-	94.75	2.41	12.56ms/2.63s
	ACMII-Snowball-2	0.1	1.00E-02	0.4	64	2	-	-	-	-	-	95.25	1.55	9.74ms/1.97s
	ACMII-Snowball-3	0.05	1.00E-02	0.6	64	3	-	-	-	-	-	94.75	3.09	11.91ms/2.42s
Film	ACM-SGC-1	0.05	5.00E-05	0.7	64	-	-	-	-	-	-	39.33	1.25	5.21ms/2.33s
	ACM-SGC-2	0.1	5.00E-05	0.7	64	-	-	-	-	-	-	40.13	1.21	12.41ms/4.87s
	ACM-GCN	0.1	5.00E-04	0.5	64	2	-	-	-	-	-	41.62	1.15	10.72ms/2.66s
	ACMII-GCN	0.1	5.00E-04	0.5	64	2	-	-	-	-	-	41.24	1.16	10.51ms/2.44s
	ACM-GCNII	0.01	0.00E+00	0.5	64	3	-	-	-	1.5	0.2	41.37	1.37	13.65ms/2.74s
	ACM-GCNII*	0.01	1.00E-05	0.5	64	3	-	-	-	1.5	0.1	41.27	1.24	14.98ms/3.01s
	ACM-Snowball-2	0.1	5.00E-03	0	64	2	-	-	-	-	-	41.4	1.23	10.30ms/2.08s
	ACM-Snowball-3	0.05	1.00E-02	0	64	3	-	-	-	-	-	41.27	0.8	16.43ms/3.52s
	ACMII-Snowball-2	0.1	5.00E-03	0	64	2	-	-	-	-	-	41.1	0.75	10.74ms/2.19s
	ACMII-Snowball-3	0.05	5.00E-03	0.2	64	3	-	-	-	-	-	40.31	1.6	16.31ms/3.29s
Chameleon	ACM-SGC-1	0.1	5.00E-06	0.9	64	-	-	-	-	-	-	63.68	1.62	5.41ms/1.21s
	ACM-SGC-2	0.1	5.00E-06	0.9	64	-	-	-	-	-	-	60.48	1.55	7.86ms/1.81s
	ACM-GCN	0.01	5.00E-05	0.8	64	2	-	-	-	-	-	68.18	1.67	10.55ms/3.12s
	ACMII-GCN	0.05	5.00E-05	0.7	64	2	-	-	-	-	-	68.58	1.36	10.90ms/2.39s
	ACM-GCNII	0.01	5.00E-06	0.5	64	4	-	-	-	0.5	0.1	58.73	2.52	18.31ms/3.68s
	ACM-GCNII*	0.01	1.00E-03	0.5	64	1	-	-	-	1	0.1	61.66	2.29	6.68ms/1.40s
	ACM-Snowball-2	0.05	5.00E-05	0.7	64	2	-	-	-	-	-	68.51	1.7	9.92ms/2.06s
	ACM-Snowball-3	0.01	1.00E-04	0.7	64	3	-	-	-	-	-	68.4	2.05	14.49ms/3.15s
	ACMII-Snowball-2	0.1	5.00E-05	0.6	64	2	-	-	-	-	-	67.83	2.63	9.99ms/2.10s
	ACMII-Snowball-3	0.05	1.00E-04	0.7	64	3	-	-	-	-	-	67.53	2.83	15.03ms/3.29s
Squirrel	ACM-SGC-1	0.05	0.00E+00	0.9	64	-	-	-	-	-	-	46.4	1.13	6.96ms/2.16s
	ACM-SGC-2	0.05	0.00E+00	0.9	64	-	-	-	-	-	-	40.91	1.39	35.20ms/10.66s
	ACM-GCN	0.05	5.00E-06	0.6	64	2	-	-	-	-	-	58.02	1.86	14.35ms/2.98s
	ACMII-GCN	0.05	0.00E+00	0.7	64	2	-	-	-	-	-	53.76	1.63	14.08ms/3.39s
	ACM-GCNII	0.01	1.00E-05	0.5	64	4	-	-	-	0.5	0.1	40.9	1.58	20.72ms/4.17s
	ACM-GCNII*	0.01	1.00E-03	0.5	64	4	-	-	-	0.5	0.3	38.32	1.5	21.78ms/4.38s
	ACM-Snowball-2	0.05	5.00E-06	0.6	64	2	-	-	-	-	-	55.97	2.03	15.38ms/3.15s
	ACM-Snowball-3	0.01	1.00E-04	0.6	64	3	-	-	-	-	-	55.73	2.39	26.15ms/5.94s
	ACMII-Snowball-2	0.1	5.00E-06	0.6	64	2	-	-	-	-	-	53.48	0.6	15.54ms/3.19s
	ACMII-Snowball-3	0.05	5.00E-05	0.5	64	3	-	-	-	-	-	52.31	1.57	26.24ms/5.30s
Cora	ACM-SGC-1	0.01	5.00E-06	0.9	64	-	-	-	-	-	-	86.63	1.13	6.00ms/7.40s
	ACM-SGC-2	0.1	5.00E-05	0.6	64	-	-	-	-	-	-	87.64	0.99	4.85ms/1.17s
	ACM-GCN	0.1	5.00E-03	0.5	64	2	-	-	-	-	-	88.62	1.22	8.84ms/1.81s
	ACMII-GCN	0.1	5.00E-03	0.4	64	2	-	-	-	-	-	89	0.72	8.93ms/1.83s
	ACM-GCNII	0.01	1.00E-03	0.5	64	3	-	-	-	1	0.2	89.1	1.61	14.07ms/3.04s
	ACM-GCNII*	0.01	1.00E-02	0.5	64	4	-	-	-	1	0.2	89	1.35	11.36ms/2.48s
	ACM-Snowball-2	0.05	1.00E-03	0.6	64	2	-	-	-	-	-	88.83	1.49	9.34ms/1.92s
	ACM-Snowball-3	0.01	1.00E-02	0.3	64	3	-	-	-	-	-	89.59	1.58	13.33ms/2.75s
	ACMII-Snowball-2	0.1	5.00E-03	0.5	64	2	-	-	-	-	-	88.95	1.04	9.29ms/1.90s
	ACMII-Snowball-3	0.1	5.00E-03	0.5	64	3	-	-	-	-	-	89.36	1.26	14.18ms/2.89s
CiteSeer	ACM-SGC-1	0.01	5.00E-04	0.9	64	-	-	-	-	-	-	80.96	0.93	5.90ms/4.31s
	ACM-SGC-2	0.05	5.00E-04	0.9	64	-	-	-	-	-	-	80.93	1.16	5.01ms/1.42s
	ACM-GCN	0.05	5.00E-03	0.7	64	2	-	-	-	-	-	81.68	0.97	11.35ms/2.57s
	ACMII-GCN	0.05	5.00E-05	0.7	64	2	-	-	-	-	-	81.58	1.77	9.55ms/1.94s
	ACM-GCNII	0.01	1.00E-02	0.5	64	3	-	-	-	0.5	0.3	82.28	1.12	15.61ms/3.56s
	ACM-GCNII*	0.01	1.00E-02	0.5	64	3	-	-	-	0.5	0.5	81.58	1.25	15.56ms/3.61s
	ACM-Snowball-2	0.05	5.00E-03	0.7	64	2	-	-	-	-	-	81.58	1.23	11.14ms/2.50s
	ACM-Snowball-3	0.01	5.00E-03	0.9	64	3	-	-	-	-	-	81.32	0.97	15.91ms/5.36s
	ACMII-Snowball-2	0.05	5.00E-03	0.7	64	2	-	-	-	-	-	82.07	1.04	10.97ms/2.55s
	ACMII-Snowball-3	0.05	1.00E-04	0.6	64	3	-	-	-	-	-	81.56	1.15	14.95ms/3.03s
PubMed	ACM-SGC-1	0.05	5.00E-06	0.3	64	-	-	-	-	-	-	87.75	0.88	6.04ms/2.61s
	ACM-SGC-2	0.05	5.00E-05	0.1	64	-	-	-	-	-	-	88.79	0.5	8.62ms/3.18s
	ACM-GCN	0.1	5.00E-04	0.2	64	2	-	-	-	-	-	90.54	0.63	10.20ms/2.08s
	ACMII-GCN	0.1	5.00E-04	0.2	64	2	-	-	-	-	-	90.74	0.5	10.20ms/2.07s
	ACM-GCNII	0.01	1.00E-04	0.5	64</td									

Datasets	Models\Hyperparameters	lr	weight_decay	dropout	hidden	with A	results	std	average epoch time/average total time
Cornell	ACM-GCN+	0.05	1.00E-02	0.1	64	Y	94.92	2.79	16.66ms/3.37s
	ACMII-GCN+	0.05	1.00E-02	0.3	64	Y	93.93	1.05	12.55ms/2.56s
	ACM-GCN++(with xX)	0.1	5.00E-03	0.4	64	N	93.93	3.03	12.89ms/2.62s
	ACMII-GCN++(with xX)	0.05	1.00E-02	0.6	64	Y	92.62	2.57	18.25ms/3.69s
Wisconsin	ACM-GCN+	0.05	1.00E-02	0.3	64	Y	96.5	2.08	16.54ms/3.35s
	ACMII-GCN+	0.01	1.00E-02	0.1	64	N	97.5	1.25	12.09ms/2.88s
	ACM-GCN++(with xX)	0.05	1.00E-02	0.1	64	Y	96.75	1.79	18.12ms/3.66s
	ACMII-GCN++(with xX)	0.01	1.00E-02	0.1	64	Y	97.13	1.68	17.32ms/3.53s
Texas	ACM-GCN+	0.05	1.00E-03	0.3	64	N	94.92	2.79	12.05ms/2.44s
	ACMII-GCN+	0.05	1.00E-02	0.1	64	Y	96.56	2	22.63 ms/4.58s
	ACM-GCN++(with xX)	0.05	5.00E-04	0.2	64	N	95.41	2.82	13.20ms/2.67s
	ACMII-GCN++(with xX)	0.05	5.00E-04	0.1	64	N	94.75	2.91	12.82ms/2.60s
Film	ACM-GCN+	0.01	1.00E-03	0.8	64	N	41.79	1.01	13.57ms/3.59s
	ACMII-GCN+	0.1	5.00E-05	0.7	64	N	41.86	1.48	13.38ms/3.59s
	ACM-GCN++(with xX)	0.002	5.00E-03	0.9	64	N	41.5	1.54	13.76ms/2.77s
	ACMII-GCN++(with xX)	0.002	5.00E-03	0.9	64	N	41.66	1.42	13.67ms/2.77s
Chameleon	ACM-GCN+	0.002	1.00E-03	0.4	64	Y	76.08	2.13	18.19ms/8.60s
	ACMII-GCN+	0.1	1.00E-04	0.7	64	Y	75.23	1.72	17.39ms/3.57s
	ACM-GCN++(with xX)	0.1	5.00E-05	0.8	64	Y	75.51	1.58	18.69ms/4.17s
	ACMII-GCN++(with xX)	0.01	1.00E-04	0.8	64	Y	75.93	1.71	18.70ms/4.53s
Squirrel	ACM-GCN+	0.01	1.00E-04	0.6	64	Y	69.26	1.11	24.71ms/4.97s
	ACMII-GCN+	0.01	1.00E-04	0.6	64	Y	68.56	1.33	21.21ms/4.26s
	ACM-GCN++(with xX)	0.002	1.00E-03	0.7	64	Y	69.81	1.11	22.14ms/5.34s
	ACMII-GCN++(with xX)	0.002	1.00E-04	0.7	64	Y	69.98	1.53	21.78ms/4.38s
Cora	ACM-GCN+	0.1	5.00E-03	0.3	64	Y	89.75	1.16	17.29ms/3.52s
	ACMII-GCN+	0.1	5.00E-03	0.5	64	Y	89.33	0.81	18.08ms/3.69s
	ACM-GCN++(with xX)	0.05	5.00E-03	0.4	64	Y	89.18	1.11	18.21ms/3.69s
	ACMII-GCN++(with xX)	0.1	1.00E-02	0.1	64	Y	89.47	1.08	18.53ms/3.76s
CiteSeer	ACM-GCN+	0.1	1.00E-05	0.5	64	N	81.65	1.48	12.44ms/2.50s
	ACMII-GCN+	0.002	5.00E-03	0.8	64	N	81.83	1.65	14.87ms/15.36s
	ACM-GCN++(with xX)	0.05	5.00E-03	0.3	64	N	81.87	1.38	13.35ms/2.86s
	ACMII-GCN++(with xX)	0.01	5.00E-04	0.9	64	N	81.76	1.25	14.04ms/3.88s
PubMed	ACM-GCN+	0.1	1.00E-04	0.1	64	N	90.46	0.69	15.15ms/3.09s
	ACMII-GCN+	0.1	1.00E-04	0.3	64	N	90.39	0.33	17.36 ms/3.55s
	ACM-GCN++(with xX)	0.1	1.00E-04	0.1	64	N	90.96	0.62	16.35ms/3.47s
	ACMII-GCN++(with xX)	0.1	1.00E-04	0.3	64	N	90.63	0.56	16.18ms/3.39s
Deezer-Europe	ACM-GCN+	0.002	1.00E-06	0.7	64	N	67.4	0.44	281.97ms/140.70s
	ACMII-GCN+	0.002	1.00E-04	0.8	64	N	67.3	0.48	281.48ms/140.46s
	ACM-GCN++(with xX)	0.002	1.00E-03	0.7	64	Y	67.44	0.31	332.92ms/166.13s
	ACMII-GCN++(with xX)	0.002	1.00E-05	0.8	64	N	67.5	0.53	326.09ms/162.72s

Table 12: Optimal hyperparameters for ACM(II)-GCN+ and ACM(II)-GCN++ on random 60%/20%/20% splits

Datasets	Models\Hyperparameters	lr	weight_decay	dropout	hidden	results	std	average epoch time/average total time
Cornell	ACM-SGC-1	0.01	5.00E-06	0	64	82.43	5.44	5.37ms/23.05s
	ACM-SGC-2	0.01	5.00E-06	0	64	82.43	5.44	5.93ms/25.66s
	ACM-GCN	0.05	5.00E-04	0.5	64	85.14	6.07	8.04ms/1.67s
	ACMII-GCN	0.1	1.00E-04	0	64	85.95	5.64	7.83ms/2.66s
	FAGCN	0.01	1.00E-04	0.6	64	76.76	5.87	8.80ms/7.67s
	ACM-Snowball-2	0.05	5.00E-03	0.3	64	85.41	5.43	11.50ms/2.35s
	ACM-Snowball-3	0.05	5.00E-03	0.2	64	83.24	5.38	15.06ms/3.12s
	ACMII-Snowball-2	0.1	5.00E-03	0.2	64	85.68	5.93	12.63ms/2.58s
	ACMII-Snowball-3	0.05	5.00E-03	0.2	64	82.7	4.86	14.59ms/3.06s
Wisconsin	ACM-SGC-1	0.1	5.00E-06	0	64	86.47	3.77	5.07ms/14.07s
	ACM-SGC-2	0.1	5.00E-06	0	64	86.47	3.77	5.30ms/16.05s
	ACM-GCN	0.05	1.00E-03	0.4	64	88.43	3.22	8.04ms/1.66s
	ACMII-GCN	0.01	5.00E-05	0.1	64	87.45	3.74	8.40ms/2.19s
	FAGCN	0.01	5.00E-05	0.5	64	79.61	1.59	8.61ms/5.84s
	ACM-Snowball-2	0.01	1.00E-03	0.4	64	87.06	2	12.51ms/2.60s
	ACM-Snowball-3	0.01	1.00E-02	0.1	64	86.67	4.37	14.92ms/3.15s
	ACMII-Snowball-2	0.01	5.00E-04	0.1	64	87.45	2.8	11.96ms/2.63s
	ACMII-Snowball-3	0.01	5.00E-03	0.5	64	85.29	4.23	14.87ms/3.10s
Texas	ACM-SGC-1	0.01	1.00E-05	0	64	81.89	4.53	5.34ms/19.00s
	ACM-SGC-2	0.05	1.00E-05	0	64	81.89	4.53	5.50ms/9.26s
	ACM-GCN	0.05	5.00E-04	0.5	64	87.84	4.4	9.62ms/1.99s
	ACMII-GCN	0.01	1.00E-03	0.1	64	86.76	4.75	9.98ms/2.22s
	FAGCN	0.01	1.00E-05	0	64	76.49	2.87	10.45ms/5.70s
	ACM-Snowball-2	0.01	5.00E-03	0.2	64	87.57	4.86	11.56ms/2.45s
	ACM-Snowball-3	0.01	5.00E-03	0.2	64	87.84	3.87	15.17ms/3.15s
	ACMII-Snowball-2	0.01	1.00E-03	0.2	64	86.76	4.43	11.36ms/2.30
	ACMII-Snowball-3	0.01	5.00E-03	0.6	64	85.41	6.42	15.84ms/3.48s
Film	ACM-SGC-1	0.05	5.00E-04	0	64	35.49	1.06	5.39ms/1.17s
	ACM-SGC-2	0.05	5.00E-04	0.1	64	36.04	0.83	13.22ms/3.31s
	ACM-GCN	0.01	5.00E-03	0	64	36.28	1.09	8.96ms/1.82s
	ACMII-GCN	0.01	5.00E-03	0	64	36.16	1.11	9.06ms/1.83s
	FAGCN	0.01	5.00E-05	0.4	64	34.82	1.35	15.60ms/2.51s
	ACM-Snowball-2	0.01	1.00E-02	0	64	36.89	1.18	14.77ms/3.01s
	ACM-Snowball-3	0.01	1.00E-02	0.2	64	36.82	0.94	16.57ms/3.36s
	ACMII-Snowball-2	0.01	5.00E-03	0.1	64	36.55	1.24	12.76ms/2.57s
	ACMII-Snowball-3	0.05	5.00E-03	0.3	64	36.49	1.41	16.51ms/3.49s
Chameleon	ACM-SGC-1	0.1	5.00E-06	0.9	64	63.99	1.66	5.92ms/1.74s
	ACM-SGC-2	0.1	0.00E+00	0.9	64	59.21	2.22	8.84ms/1.78s
	ACM-GCN	0.05	5.00E-04	0.7	64	66.93	1.85	8.40ms/1.71s
	ACMII-GCN	0.05	5.00E-06	0.8	64	66.91	2.55	8.90ms/2.10s
	FAGCN	0.01	5.00E-05	0	64	46.07	2.11	16.90ms/7.94s
	ACM-Snowball-2	0.01	1.00E-04	0.7	64	67.08	2.04	12.50ms/2.69s
	ACM-Snowball-3	0.01	1.00E-05	0.8	64	66.91	1.73	16.12ms/4.91s
	ACMII-Snowball-2	0.01	5.00E-05	0.8	64	66.49	1.75	12.65ms/3.42s
	ACMII-Snowball-3	0.05	5.00E-05	0.7	64	66.86	1.74	17.60ms/4.06s
Squirrel	ACM-SGC-1	0.05	5.00E-06	0.9	64	45	1.4	6.10ms/2.18s
	ACM-SGC-2	0.05	0.00E+00	0.9	64	40.02	0.96	35.75ms/9.62s
	ACM-GCN	0.05	5.00E-06	0.7	64	54.4	1.88	10.48ms/2.68s
	ACMII-GCN	0.05	5.00E-06	0.7	64	51.85	1.38	11.69ms/2.91s
	FAGCN	0	5.00E-03	0	64	30.86	0.69	10.90ms/13.91s
	ACM-Snowball-2	0.01	1.00E-04	0.7	64	52.5	1.49	17.89ms/5.78s
	ACM-Snowball-3	0.01	5.00E-05	0.7	64	53.31	1.88	22.60ms/7.53s
	ACMII-Snowball-2	0.05	5.00E-05	0.6	64	50.15	1.4	16.95ms/3.45s
	ACMII-Snowball-3	0.01	5.00E-04	0.6	64	48.87	1.23	23.52ms/4.94s
Cora	ACM-SGC-1	0.05	5.00E-05	0.7	64	86.9	1.38	4.99ms/2.40s
	ACM-SGC-2	0.1	0	0.8	64	87.69	1.07	5.16ms/1.16s
	ACM-GCN	0.01	5.00E-05	0.6	64	87.91	0.95	8.41ms/1.84s
	ACMII-GCN	0.01	1.00E-04	0.6	64	88.01	1.08	8.59ms/1.96s
	FAGCN	0.02	1.00E-04	0.5	64	88.05	1.57	9.30ms/10.64s
	ACM-Snowball-2	0.01	1.00E-03	0.5	64	87.42	1.09	12.54ms/2.72s
	ACM-Snowball-3	0.01	5.00E-06	0.9	64	87.1	0.93	15.83ms/11.33s
	ACMII-Snowball-2	0.01	1.00E-03	0.6	64	87.57	0.86	12.06ms/2.64s
	ACMII-Snowball-3	0.01	5.00E-03	0.5	64	87.16	1.01	16.29ms/3.62s
CiteSeer	ACM-SGC-1	0.05	0.00E+00	0.7	64	76.73	1.59	5.24ms/1.14s
	ACM-SGC-2	0.1	0.00E+00	0.8	64	76.59	1.69	5.14ms/1.03s
	ACM-GCN	0.01	5.00E-06	0.3	64	77.32	1.7	8.89ms/1.79s
	ACMII-GCN	0.01	5.00E-05	0.5	64	77.15	1.45	8.95ms/1.80s
	FAGCN	0.02	5.00E-05	0.4	64	77.07	2.05	10.05ms/5.69s
	ACM-Snowball-2	0.01	5.00E-05	0	64	76.41	1.38	12.87ms/2.59s
	ACM-Snowball-3	0.01	5.00E-06	0.9	64	75.91	1.57	17.40ms/11.92s
	ACMII-Snowball-2	0.01	5.00E-03	0.5	64	76.92	1.45	13.10ms/2.94s
	ACMII-Snowball-3	0.1	5.00E-05	0.9	64	76.18	1.55	17.47ms/5.88s
PubMed	ACM-SGC-1	0.05	5.00E-06	0.4	64	88.49	0.51	5.77ms/3.65s
	ACM-SGC-2	0.05	5.00E-06	0.3	64	89.01	0.6	8.50ms/5.18s
	ACM-GCN	0.01	5.00E-05	0.4	64	90	0.52	8.99ms/2.51s
	ACMII-GCN	0.01	1.00E-04	0.3	64	89.89	0.43	9.70ms/2.57s
	FAGCN	0.01	1.00E-04	0	64	88.09	1.38	10.30ms/8.75s
	ACM-Snowball-2	0.01	1.00E-03	0.3	64	89.89	0.57	15.05ms/3.11s
	ACM-Snowball-3	0.01	5.00E-03	0.1	64	89.81	0.43	20.51ms/4.63s
	ACMII-Snowball-2	0.01	5.00E-04	0.4	64	89.84	0.48	15.10ms/3.2s
	ACMII-Snowball-3	0.01	1.00E-03	0.4	64	89.73	0.52	20.46ms/4.32s

Table 13: Optimal hyperparameters for FAGCN and ACM(II)-GNNs on fixed 48%/32%/20% splits

Datasets	Models/Hyperparameters	lr	weight_decay	dropout	hidden	with A	results	std	average epoch time/average total time
Cornell	ACM-GCN+	0.05	1.00E-03	0.1	64	N	85.68	4.84	10.86ms/2.28s
	ACMII-GCN+	0.05	5.00E-03	0	64	Y	85.41	5.3	14.42ms/2.97s
	ACM-GCN++	0.01	5.00E-04	0.1	64	N	85.68	5.8	14.15ms/3.17s
	ACMII-GCN++	0.01	5.00E-03	0.3	64	N	86.49	6.73	14.11ms/3.19s
Wisconsin	ACM-GCN+	0.01	1.00E-03	0.1	64	Y	88.43	2.39	14.50ms/3.18s
	ACMII-GCN+	0.01	5.00E-03	0.3	64	Y	88.04	3.66	17.71ms/3.75s
	ACM-GCN++	0.05	5.00E-03	0.1	64	Y	88.24	3.16	20.61ms/4.29s
	ACMII-GCN++	0.01	5.00E-03	0.2	64	Y	88.43	3.66	18.28ms/3.75s
Texas	ACM-GCN+	0.01	5.00E-04	0.2	64	Y	88.38	3.64	22.63ms/4.63s
	ACMII-GCN+	0.05	1.00E-02	0.4	64	Y	88.11	3.24	16.92ms/3.44s
	ACM-GCN++	0.01	5.00E-03	0.3	64	Y	88.38	3.43	20.69ms/4.25s
	ACMII-GCN++	0.01	5.00E-03	0.6	64	Y	88.38	3.43	18.58ms/3.84s
Film	ACM-GCN+	0.05	5.00E-03	0	64	N	36.13	1.19	18.33ms/3.68s
	ACMII-GCN+	0.05	5.00E-03	0	64	N	35.95	1.33	19.07ms/3.83s
	ACM-GCN++	0.01	5.00E-03	0	64	N	37.31	1.09	18.57ms/3.73s
	ACMII-GCN++	0.01	5.00E-03	0	64	N	36.68	1.35	15.79ms/3.17s
Chameleon	ACM-GCN+	0.05	1.00E-04	0.7	64	Y	74.23	2.25	25.31ms/5.14s
	ACMII-GCN+	0.05	1.00E-04	0.7	64	Y	74.3	2.03	25.04ms/5.04s
	ACM-GCN++	0.002	5.00E-04	0.8	64	Y	74.3	2.23	19.44ms/8.58s
	ACMII-GCN++	0.01	1.00E-04	0.8	64	Y	74.45	1.34	21.24ms/4.92s
Squirrel	ACM-GCN+	0.002	1.00E-04	0.6	64	Y	66.06	2.16	36.96ms/7.82s
	ACMII-GCN+	0.01	5.00E-04	0.8	64	Y	65.95	1.74	35.56ms/9.18s
	ACM-GCN++	0.01	1.00E-04	0.8	64	Y	66.45	1.83	26.34ms/6.20s
	ACMII-GCN++	0.002	5.00E-04	0.8	64	Y	66.75	1.82	24.55ms/10.49s
Cora	ACM-GCN+	0.002	0.00E+00	0.6	64	N	88.05	0.99	15.21ms/5.00s
	ACMII-GCN+	0.002	5.00E-05	0.7	64	Y	88.19	1.17	13.74ms/5.67s
	ACM-GCN++	0.002	5.00E-06	0.7	64	N	88.11	0.96	14.59ms/5.05s
	ACMII-GCN++	0.002	5.00E-05	0.7	64	N	88.25	0.96	15.75ms/5.87s
CiteSeer	ACM-GCN+	0.01	5.00E-05	0.3	64	N	77.67	1.19	17.36ms/3.49s
	ACMII-GCN+	0.01	5.00E-03	0.2	64	Y	77.2	1.61	22.99ms/4.74s
	ACM-GCN++	0.002	5.00E-06	0.6	64	N	77.46	1.65	14.51ms/3.88s
	ACMII-GCN++	0.01	5.00E-05	0.6	64	N	77.12	1.58	18.69ms/3.76s
PubMed	ACM-GCN+	0.05	5.00E-05	0.3	64	N	89.82	0.41	24.63ms/4.95s
	ACMII-GCN+	0.01	1.00E-04	0.3	64	N	89.78	0.49	25.10ms/5.61s
	ACM-GCN++	0.01	5.00E-05	0.3	64	N	89.65	0.58	18.36ms/3.76s
	ACMII-GCN++	0.002	5.00E-06	0.4	64	N	89.71	0.48	16.98ms/9.44s

Table 14: Optimal hyperparameters for ACM(II)-GCN+ and ACM(II)-GCN++ on fixed 48%/32%/20% splits

D Experimental Setup and Further Discussion on Synthetic Graphs

D.1 Detailed Description of Data Generation Process

- For each node v , we first randomly generate its degree d_v .
- Given d_v , for any h , we sample hd_v intra-class edges and $(1 - h)d_v$ inter-class edges.

More specifically in our synthetic experiments, for a given h ,

- we generate node degree d_v for nodes in each class from multinomial distribution with `numpy.random.multinomial(800/h, numpy.ones(400)/400, size=1)[0]`.
- For a sampled d_v , we generate intra-class edges from (does not include self-loop) `numpy.random.multinomial(hd_v, numpy.ones(399)/399, size=1)[0]` and inter-class edges from `numpy.random.multinomial((1-h) d_v, numpy.ones(1600)/1600, size=1)[0]`.

For each generated graph, we calculate their H_{node} , H_{class} , H_{agg}^M . Then, we reorder the value of the metrics in ascend order for x-axis and plot the corresponding test accuracy.

Here is a simplified example of how we draw Figure 2. Suppose we generate 3 graphs with $H_{\text{edge}} = 0.1, 0.5, 0.9$, the test accuracy of GCN on these 3 synthetic graphs are 0.8, 0.5, 0.9. For the generated graphs, we calculate their H_{agg}^M , and suppose we get $H_{\text{agg}}^M = 0.7, 0.4, 0.8$. Then we will draw the performance of GCN under H_{agg}^M with ascend x-axis order [0.4, 0.7, 0.8] and the corresponding reordered y-axis is [0.5, 0.8, 0.9]. Other figures are drawn with the same process.

D.2 Model Comparison on Synthetic Graphs

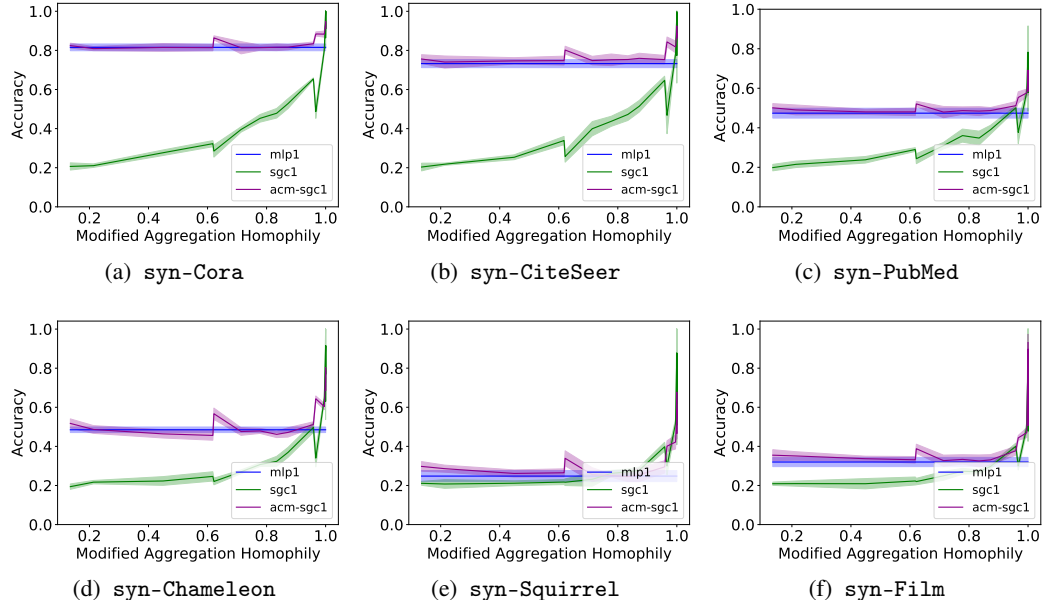


Figure 10: Comparison of test accuracy (mean \pm std) of MLP-1, SGC-1 and ACM-SGC-1 on synthetic datasets

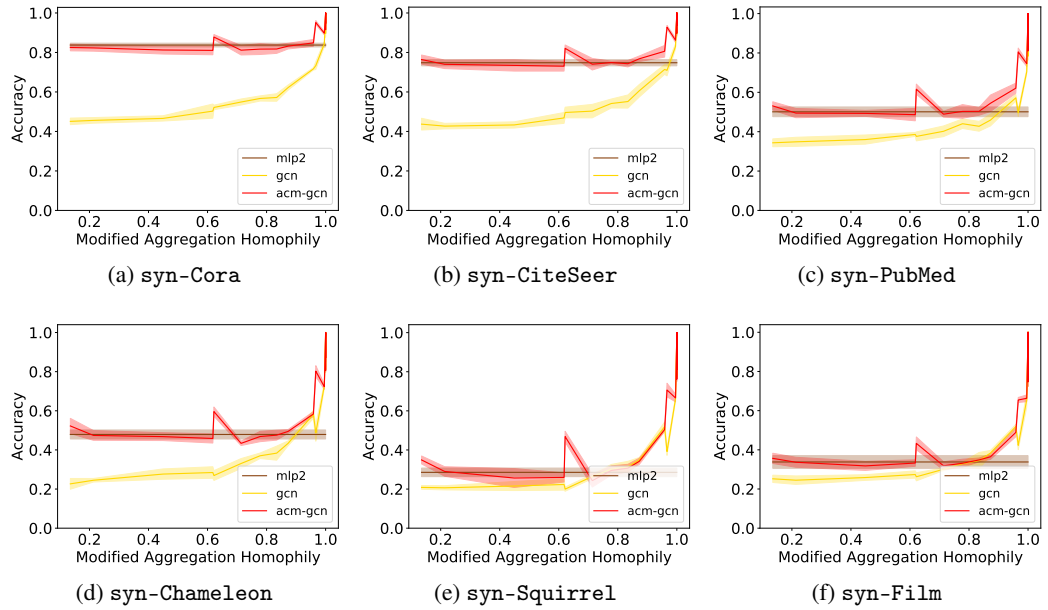


Figure 11: Comparison of test accuracy (mean \pm std) of MLP-2, GCN and ACM-GCN on synthetic datasets

In order to separate the effects of nonlinearity and graph structure, we compare SGC with 1 hop ($sgc-1$) with MLP-1 (linear model). For GCN which includes nonlinearity, we use MLP-2 as its corresponding graph-agnostic baseline model. We train the above GNN models, graph-agnostic baseline models and ACM-GNN models on all synthetic datasets and plot the mean test accuracy with standard deviation on each dataset. From Figure 10 and Figure 11, we can see that on each $H_{\text{agg}}^M(\mathcal{G})$ level, ACM-GNNs will not underperform baseline GNNs and the graph-agnostic models. But when $H_{\text{agg}}^M(\mathcal{G})$ is small, baseline GNNs will be outperformed by graph-agnostic models by a large margin. This demonstrate that the ACM framework can help GNNs to perform well on harmful graphs while keep competitive on less harmful graphs.

D.3 Further Discussion of Aggregation Homophily on Regular Graphs

We notice that in Figure 2(a), the performance of SGC-1 and GCN both have a turning point, *i.e.*, when $H_{\text{edge}}(\mathcal{G})$ is smaller than a certain value, the performance will get better instead of getting worse. With some extra restriction on node degree in data generation process, we find that this interesting phenomenon can be theoretically explained by the following proposition 1 based on our proposed similarity matrix which can verify the usefulness of $H_{\text{agg}}^M(\mathcal{G})$. We first generate regular graphs, *i.e.*, each node has the same degree, as follows,

Generate Synthetic Regular Graphs We first generate 180 graphs in total with 18 edge homophily levels varied from 0.05 to 0.9, each corresponding to 10 graphs. For every generated graph, we have 5 classes with 400 nodes in each class. For each node, we randomly generate 10 intra-class edges and $\lceil \frac{10}{H_{\text{edge}}(\mathcal{G})} - 10 \rceil$ inter-class edges. The features of nodes in each class are sampled from node features in the corresponding class of the base dataset. Nodes are randomly split into 60%/20%/20% for train/validation/test. We train 1-hop SGC ($sgc-1$) [41] and GCN [19] on synthetic data (see Appendix C.1 for hyperparameter searching range). For each value of $H_{\text{edge}}(\mathcal{G})$, we take the average test accuracy and standard deviation of runs over 10 generated graphs. We plot the performance curves in Figure 12.

From Figure 12 we can see that the turning point is a bit less than 0.2. We derive the following proposition for d -regular graph to explain and predict it.

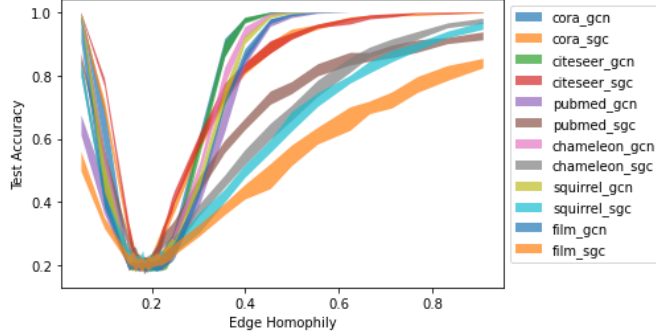


Figure 12: Synthetic experiments for edge homophily on regular graphs.

Proposition 1. (See Appendix F for proof). Suppose there are C classes in the graph \mathcal{G} and \mathcal{G} is a d -regular graph (each node has d neighbors). Given d , edges for each node are *i.i.d.* generated, such that each edge of any node has probability h to connect with nodes in the same class and probability $1 - h$ to connect with nodes in different classes. Let the aggregation operator $\hat{A} = \hat{A}_{\text{rw}}$. Then, for nodes v, u_1 and u_2 , where $Z_{u_1,:} = Z_{v,:}$ and $Z_{u_2,:} \neq Z_{v,:}$, we have

$$g(h) \equiv \mathbb{E} \left(S(\hat{A}, Z)_{v, u_1} \right) - \mathbb{E} \left(S(\hat{A}, Z)_{v, u_2} \right) = \left(\frac{(C-1)(hd+1) - (1-h)d}{(C-1)(d+1)} \right)^2 \quad (12)$$

and the minimum of $g(h)$ is reached at

$$h = \frac{d+1-C}{Cd} = \frac{d_{\text{intra}}/h + 1 - C}{C(d_{\text{intra}}/h)} \Rightarrow h = \frac{d_{\text{intra}}}{Cd_{\text{intra}} + C - 1}$$

where $d_{\text{intra}} = dh$, which is the expected number of neighbors of a node that have the same label as the node.

The value of $g(h)$ in equation 12 is the expected differences of the similarity values between nodes in the same class as v and nodes in other classes. $g(h)$ is strongly related to the definition of aggregation homophily and its minimum potentially implies the turning point of performance curves. In the synthetic experiments, we have $d_{\text{intra}} = 10, C = 5$ and the minimum of $g(h)$ is reached at $h = 5/27 \approx 0.1852$, which corresponds to the lowest point in the performance curve in Figure 12. In other words, the $H_{\text{edge}}(\mathcal{G})$ where SGC-1 and GCN perform worst is where $g(h)$ gets the smallest value, instead of the point with the smallest edge homophily value, *i.e.*, $H_{\text{edge}}(\mathcal{G}) = 0$. This reveals the advantage of $H_{\text{agg}}(\mathcal{G})$ over $H_{\text{edge}}(\mathcal{G})$ by taking use of the similarity matrix.

E Details of Gradient Calculation in equation 6

E.1 Derivation in Matrix Form

This derivation is similar to [30].

In output layer, we have

$$Y = \text{softmax}(\hat{A}XW) \equiv \text{softmax}(Y') = (\exp(Y')\mathbf{1}_C\mathbf{1}_C^T)^{-1} \odot \exp(Y') > 0$$

$$\mathcal{L} = -\text{trace}(Z^T \log Y)$$

where $\mathbf{1}_C \in \mathcal{R}^{C \times 1}$, $(\cdot)^{-1}$ is point-wise inverse function and each element of Y is positive. Then

$$d\mathcal{L} = -\text{trace}(Z^T((Y)^{-1} \odot dY)) = -\text{trace}(Z^T((\text{softmax}(Y'))^{-1} \odot d \text{softmax}(Y')))$$

Note that

$$\begin{aligned}
d \text{softmax}(Y') &= -(\exp(Y') \mathbf{1}_C \mathbf{1}_C^T)^{-2} \odot [(\exp(Y') \odot dY') \mathbf{1}_C \mathbf{1}_C^T] \odot \exp(Y') \\
&\quad + (\exp(Y') \mathbf{1}_C \mathbf{1}_C^T)^{-1} \odot (\exp(Y') \odot dY') \\
&= -\text{softmax}(Y') \odot (\exp(Y') \mathbf{1}_C \mathbf{1}_C^T)^{-1} \odot [(\exp(Y') \odot dY') \mathbf{1}_C \mathbf{1}_C^T] \\
&\quad + \text{softmax}(Y') \odot dY' \\
&= \text{softmax}(Y') \odot \left(-(\exp(Y') \mathbf{1}_C \mathbf{1}_C^T)^{-1} \odot [(\exp(Y') \odot dY') \mathbf{1}_C \mathbf{1}_C^T] + dY' \right)
\end{aligned}$$

Then,

$$\begin{aligned}
d\mathcal{L} &= -\text{trace} \left(Z^T \left((\text{softmax}(Y'))^{-1} \odot \left[\text{softmax}(Y') \odot \left(-(\exp(Y') \mathbf{1}_C \mathbf{1}_C^T)^{-1} \right. \right. \right. \right. \\
&\quad \left. \left. \left. \left. \odot [(\exp(Y') \odot dY') \mathbf{1}_C \mathbf{1}_C^T] + dY' \right) \right] \right) \right) \\
&= -\text{trace} \left(Z^T \left(-(\exp(Y') \mathbf{1}_C \mathbf{1}_C^T)^{-1} \odot [(\exp(Y') \odot dY') \mathbf{1}_C \mathbf{1}_C^T] + dY' \right) \right) \\
&= \text{trace} \left(\left(\left(Z \odot (\exp(Y') \mathbf{1}_C \mathbf{1}_C^T)^{-1} \right) \mathbf{1}_C \mathbf{1}_C^T \right)^T [\exp(Y') \odot dY'] - Z^T dY' \right) \\
&= \text{trace} \left(\left(\exp(Y') \odot \left(\left(Z \odot (\exp(Y') \mathbf{1}_C \mathbf{1}_C^T)^{-1} \right) \mathbf{1}_C \mathbf{1}_C^T \right) \right)^T dY' - Z^T dY' \right) \\
&= \text{trace} \left(\left(\exp(Y') \odot (\exp(Y') \mathbf{1}_C \mathbf{1}_C^T)^{-1} \right)^T dY' - Z^T dY' \right) \\
&= \text{trace} ((\text{softmax}(Y') - Z)^T dY')
\end{aligned}$$

where the 4-th equation holds due to $\left(Z \odot (\exp(Y') \mathbf{1}_C \mathbf{1}_C^T)^{-1} \right) \mathbf{1}_C \mathbf{1}_C^T = (\exp(Y') \mathbf{1}_C \mathbf{1}_C^T)^{-1}$. Thus, we have

$$\frac{d\mathcal{L}}{dY'} = \text{softmax}(Y') - Z = Y - Z$$

For Y' and W , we have

$$dY' = \hat{A}X dW \text{ and } d\mathcal{L} = \text{trace} \left(\frac{d\mathcal{L}}{dY'}^T dY' \right) = \text{trace} \left(\frac{d\mathcal{L}}{dY'}^T \hat{A}X dW \right) = \text{trace} \left(\frac{d\mathcal{L}}{dW}^T dW \right)$$

To get $\frac{d\mathcal{L}}{dW}$ we have,

$$\frac{d\mathcal{L}}{dW} = X^T \hat{A}^T \frac{d\mathcal{L}}{dY'} = X^T \hat{A}^T (Y - Z) \quad (13)$$

E.2 Component-wise Derivation

Denote $\tilde{X} = XW$. We rewrite \mathcal{L} as follows:

$$\begin{aligned}
\mathcal{L} &= -\text{trace} \left(Z^T \log \left((\exp(Y') \mathbf{1}_C \mathbf{1}_C^T)^{-1} \odot \exp(Y') \right) \right) \\
&= -\text{trace} \left(Z^T \left(-\log(\exp(Y') \mathbf{1}_C \mathbf{1}_C^T) + Y' \right) \right) \\
&= -\text{trace} (Z^T Y') + \text{trace} (Z^T \log (\exp(Y') \mathbf{1}_C \mathbf{1}_C^T)) \\
&= -\text{trace} (Z^T \hat{A}XW) + \text{trace} (Z^T \log (\exp(Y') \mathbf{1}_C \mathbf{1}_C^T)) \\
&= -\text{trace} (Z^T \hat{A}XW) + \text{trace} (\mathbf{1}_C^T \log (\exp(Y') \mathbf{1}_C))
\end{aligned}$$

Expand \mathcal{L} component-wisely, we have

$$\begin{aligned}
\mathcal{L} &= -\sum_{i=1}^N \sum_{j \in \mathcal{N}_i} \hat{A}_{i,j} Z_{i,:} \tilde{X}_{j,:}^T + \sum_{i=1}^N \log \left(\sum_{c=1}^C \exp \left(\sum_{j \in \mathcal{N}_i} \hat{A}_{i,j} \tilde{X}_{j,c} \right) \right) \\
&= -\sum_{i=1}^N \log \left(\exp \left(\sum_{c=1}^C \sum_{j \in \mathcal{N}_i} \hat{A}_{i,j} Z_{i,c} \tilde{X}_{j,c} \right) \right) + \sum_{i=1}^N \log \left(\sum_{c=1}^C \exp \left(\sum_{j \in \mathcal{N}_i} \hat{A}_{i,j} \tilde{X}_{j,c} \right) \right) \\
&= -\sum_{i=1}^N \log \frac{\exp \left(\sum_{c=1}^C \sum_{j \in \mathcal{N}_i} \hat{A}_{i,j} Z_{i,c} \tilde{X}_{j,c} \right)}{\left(\sum_{c=1}^C \exp \left(\sum_{j \in \mathcal{N}_i} \hat{A}_{i,j} \tilde{X}_{j,c} \right) \right)}
\end{aligned}$$

Note that $\sum_{c=1}^C Z_{j,c} = 1$ for any j . Consider the derivation of \mathcal{L} over $\tilde{X}_{j',c'}$:

$$\begin{aligned}
\frac{d\mathcal{L}}{d\tilde{X}_{j',c'}} &= -\sum_{i=1}^N \frac{\sum_{c=1}^C \exp \left(\sum_{j \in \mathcal{N}_i} \hat{A}_{i,j} \tilde{X}_{j,c} \right)}{\exp \left(\sum_{c=1}^C \sum_{j \in \mathcal{N}_i} \hat{A}_{i,j} Z_{i,c} \tilde{X}_{j,c} \right)} \\
&\times \left(\frac{\left(\hat{A}_{i,j'} Z_{i,c'} \right) \exp \left(\sum_{c=1}^C \sum_{j \in \mathcal{N}_i} \hat{A}_{i,j} Z_{i,c} \tilde{X}_{j,c} \right) \left(\sum_{c=1}^C \exp \left(\sum_{j \in \mathcal{N}_i} \hat{A}_{i,j} \tilde{X}_{j,c} \right) \right)}{\left(\sum_{c=1}^C \exp \left(\sum_{j \in \mathcal{N}_i} \hat{A}_{i,j} \tilde{X}_{j,c} \right) \right)^2} \right. \\
&\quad \left. - \frac{\left(\hat{A}_{i,j'} \right) \exp \left(\sum_{c=1}^C \sum_{j \in \mathcal{N}_i} \hat{A}_{i,j} Z_{i,c} \tilde{X}_{j,c} \right) \left(\exp \left(\sum_{j \in \mathcal{N}_i} \hat{A}_{i,j} \tilde{X}_{j,c'} \right) \right)}{\left(\sum_{c=1}^C \exp \left(\sum_{j \in \mathcal{N}_i} \hat{A}_{i,j} \tilde{X}_{j,c} \right) \right)^2} \right) \\
&= -\sum_{i=1}^N \left(\frac{\left(\hat{A}_{i,j'} Z_{i,c'} \right) \left(\sum_{c=1}^C \exp \left(\sum_{j \in \mathcal{N}_i} \hat{A}_{i,j} \tilde{X}_{j,c} \right) \right) - \left(\hat{A}_{i,j'} \right) \left(\exp \left(\sum_{j \in \mathcal{N}_i} \hat{A}_{i,j} \tilde{X}_{j,c'} \right) \right)}{\left(\sum_{c=1}^C \exp \left(\sum_{j \in \mathcal{N}_i} \hat{A}_{i,j} \tilde{X}_{j,c} \right) \right)} \right) \\
&= -\sum_{i=1}^N \left(\hat{A}_{i,j'} \frac{\left(\sum_{c=1, c \neq c'}^C (Z_{i,c'}) \exp \left(\sum_{j \in \mathcal{N}_i} \hat{A}_{i,j} \tilde{X}_{j,c} \right) \right) + (Z_{i,c'} - 1) \left(\exp \left(\sum_{j \in \mathcal{N}_i} \hat{A}_{i,j} \tilde{X}_{j,c'} \right) \right)}{\left(\sum_{c=1}^C \exp \left(\sum_{j \in \mathcal{N}_i} \hat{A}_{i,j} \tilde{X}_{j,c} \right) \right)} \right) \\
&= -\sum_{i=1}^N \hat{A}_{i,j'} \left(Z_{i,c'} \hat{P}(Y_i \neq c') + (Z_{i,c'} - 1) \hat{P}(Y_i = c') \right) \\
&= -\sum_{i=1}^N \hat{A}_{i,j'} \left(Z_{i,c'} - \hat{P}(Y_i = c') \right)
\end{aligned} \tag{14}$$

Writing the above in matrix form, we have

$$\frac{d\mathcal{L}}{d\tilde{X}} = \hat{A}(Z - Y), \quad \frac{d\mathcal{L}}{d\tilde{W}} = X^T \hat{A}^T (Z - Y), \quad \Delta Y' \propto \hat{A} X X^T \hat{A}^T (Z - Y) \tag{15}$$

F Proof of Proposition 1

Proof. According to the given assumptions, for node v , we have $\hat{A}_{v,k} = \frac{1}{d+1}$, the expected number of intra-class edges is dh (here the self-loop edge introduced by \hat{A} is not counted based on the definition of edge homophily and data generation process) and inter-class edges is $(1-h)d$. Suppose there are $C \geq 2$ classes. Consider matrix $\hat{A}Z$,

Then, we have $\mathbb{E}[(\hat{A}Z)_{v,c}] = \mathbb{E}\left[\sum_{k \in \mathcal{V}} \hat{A}_{v,k} \mathbf{1}_{\{Z_{k,:} = e_c^T\}}\right] = \sum_{k \in \mathcal{V}} \frac{\mathbb{E}[\mathbf{1}_{\{Z_{k,:} = e_c^T\}}]}{d+1}$, where $\mathbf{1}$ is the indicator function.

When v is in class c , we have $\sum_{k \in \mathcal{V}} \frac{\mathbb{E}[\mathbf{1}_{\{Z_{k,:} = e_c^T\}}]}{d+1} = \frac{hd+1}{d+1}$ ($hd+1 = hd$ intra-class edges + 1 self-loop introduced by \hat{A}).

When v is not in class c , we have $\sum_{k \in \mathcal{V}} \frac{\mathbb{E}[\mathbf{1}_{\{Z_{k,:} = e_c^T\}}]}{d+1} = \frac{(1-h)d}{(C-1)(d+1)}$ ($(1-h)d$ inter-class edges uniformly distributed in the other $C-1$ classes).

For nodes v, u , we have $(\hat{A}Z)_{v,:}, (\hat{A}Z)_{u,:} \in \mathbb{R}^C$ and since elements in $\hat{A}_{v,k}$ and $\hat{A}_{u,k'}$ are independently generated for all $k, k' \in \mathcal{V}$, we have

$$\begin{aligned} \mathbb{E}[(\hat{A}Z)_{v,c}(\hat{A}Z)_{u,c}] &= \mathbb{E}\left[\left(\sum_{k \in \mathcal{V}} \hat{A}_{v,k} \mathbf{1}_{\{Z_{k,:} = e_c^T\}}\right)\left(\sum_{k' \in \mathcal{V}} \hat{A}_{u,k'} \mathbf{1}_{\{Z_{k',:} = e_c^T\}}\right)\right] \\ &= \mathbb{E}\left[\left(\sum_{k \in \mathcal{V}} \hat{A}_{v,k} \mathbf{1}_{\{Z_{k,:} = e_c^T\}}\right)\right] \mathbb{E}\left[\left(\sum_{k' \in \mathcal{V}} \hat{A}_{u,k'} \mathbf{1}_{\{Z_{k',:} = e_c^T\}}\right)\right] \end{aligned}$$

Thus,

$$\begin{aligned} \mathbb{E}[S(\hat{A}, Z)_{v,u}] &= \mathbb{E}[<(\hat{A}Z)_{v,:}, (\hat{A}Z)_{u,:}>] = \sum_c \mathbb{E}\left[\left(\sum_{k \in \mathcal{V}} \hat{A}_{v,k} \mathbf{1}_{\{Z_{k,:} = e_c^T\}}\right)\right] \mathbb{E}\left[\left(\sum_{k' \in \mathcal{V}} \hat{A}_{u,k'} \mathbf{1}_{\{Z_{k',:} = e_c^T\}}\right)\right] \\ &= \begin{cases} \left(\frac{hd+1}{d+1}\right)^2 + \frac{((1-h)d)^2}{(C-1)(d+1)^2}, & u, v \text{ are in the same class} \\ \frac{2(hd+1)(1-h)d}{(C-1)(d+1)^2} + \frac{(C-2)(1-h)^2d^2}{(C-1)^2(d+1)^2}, & u, v \text{ are in different classes} \end{cases} \end{aligned}$$

For nodes u_1, u_2 , and v , where $Z_{u_1,:} = Z_{v,:}$ and $Z_{u_2,:} \neq Z_{v,:}$,

$$\begin{aligned} g(h) &\equiv \mathbb{E}[S(\hat{A}, Z)_{v,u_1}] - \mathbb{E}[S(\hat{A}, Z)_{v,u_2}] \quad (16) \\ &= \frac{(C-1)^2(hd+1)^2 + (C-1)[(1-h)d]^2 - (C-1)(2(hd+1)(1-h)d) - (C-2)[(1-h)d]^2}{(C-1)^2(d+1)^2} \\ &= \left(\frac{(C-1)(hd+1) - (1-h)d}{(C-1)(d+1)}\right)^2 \end{aligned}$$

Setting $g(h) = 0$, we obtain the optimal h :

$$h = \frac{d+1-C}{Cd} \quad (17)$$

For the data generation process in the synthetic experiments, we fix d_{intra} , then $d = d_{\text{intra}}/h$, which is a function of h . We change d in equation 17 to d_{intra}/h , leading to

$$h = \frac{d_{\text{intra}}/h + 1 - C}{Cd_{\text{intra}}/h} \quad (18)$$

It is easy to observe that h satisfying equation 18 still makes $g(h) = 0$, when d in $g(h)$ is replaced by d_{intra}/h . From equation 18 we obtain the optimal h in terms of d_{intra} :

$$h = \frac{d_{\text{intra}}}{Cd_{\text{intra}} + C - 1}$$

□

F.1 An Extension of Proposition 1

Base on the definition of aggregation similarity, we have

$$\begin{aligned} S_{\text{agg}}(S(\hat{A}, Z)) &= \frac{\left| \left\{ v \mid \text{Mean}_u(\{S(\hat{A}, Z)_{v,u} | Z_{u,:} = Z_{v,:}\}) \geq \text{Mean}_u(\{S(\hat{A}, Z)_{v,u} | Z_{u,:} \neq Z_{v,:}\}) \right\} \right|}{|\mathcal{V}|} \\ &= \frac{\sum_{v \in \mathcal{V}} \mathbf{1}_{\{\text{Mean}_u(\{S(\hat{A}, Z)_{v,u} | Z_{u,:} = Z_{v,:}\}) \geq \text{Mean}_u(\{S(\hat{A}, Z)_{v,u} | Z_{u,:} \neq Z_{v,:}\})\}}}{|\mathcal{V}|} \end{aligned}$$

Then,

$$\begin{aligned} \mathbb{E}(S_{\text{agg}}(S(\hat{A}, Z))) &= \mathbb{E} \left(\frac{\sum_{v \in \mathcal{V}} \mathbf{1}_{\{\text{Mean}_u(\{S(\hat{A}, Z)_{v,u} | Z_{u,:} = Z_{v,:}\}) \geq \text{Mean}_u(\{S(\hat{A}, Z)_{v,u} | Z_{u,:} \neq Z_{v,:}\})\}}}{|\mathcal{V}|} \right) \\ &= \frac{\sum_{v \in \mathcal{V}} \mathbb{P}(\text{Mean}_u(\{S(\hat{A}, Z)_{v,u} | Z_{u,:} = Z_{v,:}\}) \geq \text{Mean}_u(\{S(\hat{A}, Z)_{v,u} | Z_{u,:} \neq Z_{v,:}\}))}{|\mathcal{V}|} \\ &= \mathbb{P}(\text{Mean}_u(\{S(\hat{A}, Z)_{v,u} | Z_{u,:} = Z_{v,:}\}) - \text{Mean}_u(\{S(\hat{A}, Z)_{v,u} | Z_{u,:} \neq Z_{v,:}\}) \geq 0) \end{aligned}$$

Consider the random variable

$$RV = \text{Mean}_u(\{S(\hat{A}, Z)_{v,u} | Z_{u,:} = Z_{v,:}\}) - \text{Mean}_u(\{S(\hat{A}, Z)_{v,u} | Z_{u,:} \neq Z_{v,:}\})$$

Since RV is symmetrically distributed and under the conditions in proposition 1, its expectation is $\mathbb{E}[RV] = g(h)$ as showed in equation 16. Since the minimum of $g(h)$ is 0 and RV is symmetrically distributed, we have $\mathbb{P}(RV \geq 0) \geq 0.5$ and this can explain why $H_{\text{agg}}(\mathcal{G})$ is always greater than 0.5 in many real-world tasks.

G Proof of Theorem 1

Proof. Define $W_v^c = (\hat{A}Z)_{v,c}$. Then,

$$W_v^c = \sum_{k \in \mathcal{V}} \hat{A}_{v,k} \mathbf{1}_{\{Z_{k,:} = e_c^T\}} \in [0, 1], \quad \sum_{c=1}^C W_v^c = 1$$

Note that

$$S(I - \hat{A}, Z) = (I - \hat{A})ZZ^T(I - \hat{A})^T = ZZ^T + \hat{A}ZZ^T\hat{A}^T - \hat{A}ZZ^T - ZZ^T\hat{A}^T \quad (19)$$

For any node v , let the class v belongs to be denoted by c_v . For two nodes v, u , if $Z_{v,:} \neq Z_{u,:}$, we have

$$\begin{aligned} (ZZ^T)_{v,u} &= 0 \\ (\hat{A}ZZ^T\hat{A}^T)_{v,u} &= \sum_{c=1}^C W_v^c W_u^c \\ (\hat{A}ZZ^T)_{v,u} &= W_v^{c_u} \\ (ZZ^T\hat{A}^T)_{v,u} &= (\hat{A}ZZ^T)_{u,v} = W_u^{c_v} \end{aligned}$$

Then, from equation 19 it follows that

$$(S(I - \hat{A}, Z))_{v,u} = \sum_{c=1}^C W_v^c W_u^c - W_v^{c_u} - W_u^{c_v}$$

When $C = 2$,

$$S(I - \hat{A}, Z)_{v,u} = W_v^{c_u} (W_u^{c_u} - 1) + W_u^{c_v} (W_v^{c_v} - 1) \leq 0$$

If $Z_{v,:} = Z_{u,:}$, i.e., $c_v = c_u$, we have

$$\begin{aligned}
 (ZZ^T)_{v,u} &= 1 \\
 (\hat{A}ZZ^T\hat{A}^T)_{v,u} &= \sum_{c=1}^C W_v^c W_u^c \\
 (\hat{A}ZZ^T)_{v,u} &= W_v^{c_v} \\
 (ZZ^T\hat{A}^T)_{v,u} &= (\hat{A}ZZ^T)_{u,v} = W_u^{c_u} = W_v^{c_v}
 \end{aligned}$$

Then, from equation 19 it follows that

$$\begin{aligned}
 S(I - \hat{A}, Z)_{v,u} &= 1 + \sum_{c=1}^C W_v^c W_u^c - W_v^{c_v} - W_u^{c_v} \\
 &= \sum_{\substack{c=1, c \neq c_v}}^C W_v^c W_u^c + 1 + W_v^{c_v} W_u^{c_v} - W_v^{c_v} - W_u^{c_v} \\
 &= \sum_{\substack{c=1, c \neq c_v}}^C W_v^c W_u^c + (1 - W_v^{c_v})(1 - W_u^{c_v}) \geq 0
 \end{aligned}$$

Thus, if $C = 2$, for any $v \in \mathcal{V}$, if $Z_{u,:} \neq Z_{v,:}$, we have $S(I - \hat{A}, Z)_{v,u} \leq 0$; if $Z_{u,:} = Z_{v,:}$, we have $S(I - \hat{A}, Z)_{v,u} \geq 0$. Apparently, the two conditions in equation 10 are satisfied. Thus v is diversification distinguishable and $\text{DD}_{\hat{A},X}(\mathcal{G}) = 1$. The theorem is proved. \square

H Discussion of the Limitations of Diversification Operation

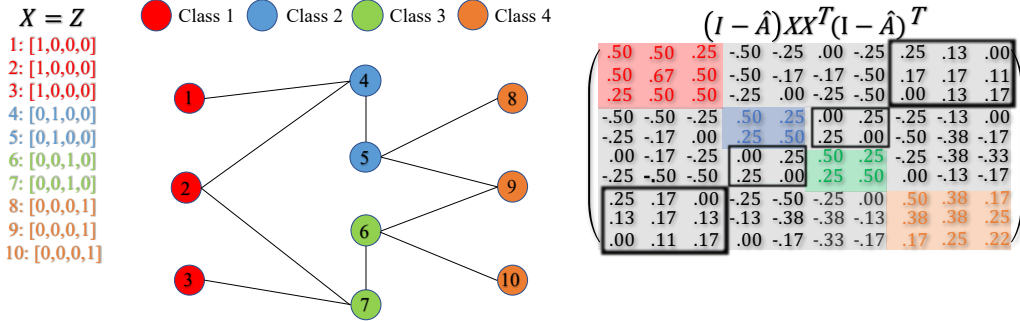


Figure 13: Example of the case (the area in black box) that HP filter does not work well for harmful heterophily

From the black box area of $S(I - \hat{A}, X)$ in the example in Figure 13 we can see that nodes in class 1 and 4 assign non-negative weights to each other although there is no edge between them; nodes in class 2 and 3 assign non-negative weights to each other as well. This is because the surrounding differences of class 1 are similar as class 4, so are class 2 and 3. In real-world applications, when nodes in several small clusters connect to a large cluster, the surrounding differences of the nodes in the small clusters will become similar. In such case, HP filter are not able to distinguish the nodes from different small clusters.

I The Similarity, Homophily and $\text{DD}_{\hat{A},X}(\mathcal{G})$ Metrics and Their Estimations

Firstly, we would like to clarify that, for each curve in the synthetic experiments, the node features are fixed and we only change the homophily values. But in real-world tasks, different datasets have different features and aggregated features. Thus, to get more instructive information for different datasets and compare them, we need to consider more metrics, e.g. feature-label consistency and

aggregated-feature-label consistency. With the similarity score of the features $S_{\text{agg}}(S(I, X))$ and aggregated features $S_{\text{agg}}(S(\hat{A}, X))$ listed in Table 15, our methods open up a new perspective on analyzing and comparing the performance of graph-agnostic models and graph-aware models in real-world tasks. Here are 2 examples.

Example 1: People observe that GCN (graph-aware model) underperforms MLP-2 (graph-agnostic model) on *Cornell*, *Wisconsin*, *Texas*, *Film* and people commonly believe that the bad graph structure (low H_{edge} , H_{node} , H_{class} values) is the reason for performance degradation. But based on the high aggregation homophily values, the graph structure inconsistency is not the main cause of the performance degradation. And from Table 15 we can see that the $S_{\text{agg}}(S(\hat{A}, X))$ for those 4 datasets are lower than their corresponding $S_{\text{agg}}(S(I, X))$, which implies that it is the aggregated-feature-label inconsistency that causes the performance degradation, i.e. the aggregation step actually decrease the quality of node features rather than making them more distinguishable.

For the rest 5 datasets *Chameleon*, *Squirrel*, *Cora*, *CiteSeer*, *PubMed*, we all have $S_{\text{agg}}(S(\hat{A}, X))$ larger than $S_{\text{agg}}(S(I, X))$ except *PubMed*, which means the aggregated features have higher quality than raw features. We can see that the proposed metrics are much more instructive than the existing ones.

Example 2: According to H_{edge} , H_{node} , H_{class} , the value for *Chameleon*, and *Squirrel* are extremely low indicating graph structure are bad for GNNs. But on contrary, GCN outperforms MLP-2 on those 2 datasets. Traditional homophily metrics fail to explain such phenomenon but our method can give an explanation from different angles: For Chameleon, its modified aggregation homophily is not low and its $S_{\text{agg}}(S(\hat{A}, X))$ is higher than its $S_{\text{agg}}(S(I, X))$, which means its graph-label consistency together with aggregated-feature-label consistency help the graph-aware model obtain the performance gain; for Squirrel, its modified aggregation homophily is low but its $S_{\text{agg}}(S(\hat{A}, X))$ is higher than its $S_{\text{agg}}(S(I, X))$, which means although its graph-label consistency is bad, the aggregated-feature-label consistency is the key factor to help the graph-aware model perform better.

We also need to point out that (modified) aggregation similarity score, $S_{\text{agg}}(S(\hat{A}, X))$ and $S_{\text{agg}}(S(I, X))$ are not deciding values because they do not consider the nonlinear structure in the features. In practice, a low score does not tell us the GNN models will definitely perform bad.

	Cornell	Wisconsin	Texas	Film	Chameleon	Squirrel	Cora	CiteSeer	PubMed
$H_{\text{agg}}(\mathcal{G})$	0.9016	0.8884	0.847	0.8411	0.805	0.6783	0.9952	0.9913	0.9716
$S_{\text{agg}}(S(\hat{A}, X))$	0.8251	0.7769	0.6557	0.5118	0.8292	0.7216	0.9439	0.9393	0.8623
$S_{\text{agg}}(S(I, X))$	0.9672	0.8287	0.9672	0.5405	0.7931	0.701	0.9103	0.9315	0.8823
$DD_{\hat{A}, X}(\mathcal{G})$	0.3497	0.6096	0.459	0.3279	0.3109	0.2711	0.2681	0.4124	0.1889
$\hat{H}_{\text{agg}}(\mathcal{G})$	0.9046 ± 0.0282	0.9147 ± 0.0260	0.8596 ± 0.0299	0.8451 ± 0.0041	0.8041 ± 0.0078	0.6788 ± 0.0077	0.9959 ± 0.0011	0.9907 ± 0.0015	0.9724 ± 0.0015
$\hat{S}_{\text{agg}}(S(\hat{A}, X))$	0.8266 ± 0.0526	0.8280 ± 0.0351	0.6835 ± 0.0498	0.5345 ± 0.0421	0.8433 ± 0.0070	0.7352 ± 0.0132	0.9487 ± 0.0023	0.9451 ± 0.0038	0.8626 ± 0.0021
$\hat{S}_{\text{agg}}(S(I, X))$	0.9752 ± 0.0174	0.8680 ± 0.0270	0.9661 ± 0.0336	0.5438 ± 0.0184	0.8257 ± 0.0050	0.7472 ± 0.0089	0.9204 ± 0.0044	0.9441 ± 0.0036	0.8835 ± 0.0019
$DD_{\hat{A}, X}(\mathcal{G})$	0.3936 ± 0.0663	0.6073 ± 0.0436	0.4817 ± 0.0762	0.3300 ± 0.0136	0.3329 ± 0.0151	0.3021 ± 0.0101	0.3198 ± 0.0225	0.4424 ± 0.0136	0.1919 ± 0.0046

Table 15: Additional metrics and their estimations with only training labels (mean \pm std)

Furthermore, in most real-world applications, not all labels are available to calculate the dataset statistics. Thus, we randomly split the data into 60%/20%/20% for training/validation/test, and only use the training labels for the estimation of the statistics. We repeat each estimation for 10 times and report the mean with standard deviation. The results are shown in table 15.

Analysis From the reported results we can see that the estimations are accurate and the errors are within the acceptable range, which means the proposed metrics and similarity scores can be accurately estimated with a subset of labels and this is important for real-world applications.

J A Detailed Explanation of the Differences Between ACM(II)-GNNs and GPRGNN, FAGCN

Differences with GPRGNN [8]:

- *GPRGNN does not feed distinct **node-wise feature transformation** to different "multi-scale channels"*

We first rewrite GPRGNN as

$$\mathbf{Z} = \sum_{k=0}^K \gamma_k \mathbf{H}^{(k)} = \sum_{k=0}^K \gamma_k I \mathbf{H}^{(k)} = \sum_{k=0}^K \text{diag}(\gamma_k, \gamma_k, \dots, \gamma_k) \mathbf{H}^{(k)}, \text{ where } \mathbf{H}^{(k)} = \hat{A}_{\text{sym}} \mathbf{H}^{(k-1)}, \mathbf{H}_{i:}^{(0)} = f_{\theta}(X_{i:}).$$

From the above equation we can see that $\mathbf{Z} = \sum_{k=0}^K \gamma_k \hat{A}_{\text{sym}}^k f_{\theta}(X_{i:})$, i.e., the **node-wise feature transformation** in GPRGNN is only learned by the same θ for all the "multi-scale channels". But in the ACM framework, different channels extract distinct information with different parameters separately.

- *GPRGNN does not have node-wise mixing mechanism.*

There is no node-wise mixing in GPRGNN. The mixing mechanism in GPRGNN is $\mathbf{Z} = \sum_{k=0}^K \text{diag}(\gamma_k, \gamma_k, \dots, \gamma_k) \mathbf{H}^{(k)}$, i.e. for each "multi-scale channel k ", all nodes share the same mixing parameter γ_k . But in the ACM framework, the node-wise channel mixing can be written as $\mathbf{Z} = \sum_{k=0}^K \text{diag}(\gamma_k^1, \gamma_k^2, \dots, \gamma_k^N) \mathbf{H}^{(k)}$ where K is the number of channels, N is the number of nodes and $\gamma_k^i, i = 1, \dots, N$ are the mixing weights that are learned by node i to mix channel k . ACM and ACMII allow GNNs to learn more diverse mixing parameters in diagonal than GPRGNN and thus, have stronger expressive power than GPRGNN.

Differences with FAGCN [4]:

- *The targets of node-wise operations in ACM (channel mixing) and FAGCN (negative message passing) are different.*

Instead of using a fixed low-pass filter \hat{A} , FAGCN tries to learn a more powerful aggregator \hat{A}' based on \hat{A} by allowing negative message passing. The node-wise operation in FAGCN is similar to GAT [3] which is trying to modify the **node-wise filtering (message passing) process**, i.e. for each node i , it assigns different weights $\alpha_{ij} \in [-1, 1]$ to different neighborhood nodes (equation 7 in FAGCN paper). The goal of this node-wise operation in FAGCN is **to learn a new filter during the filtering process node-wisely**. But in ACM, the node-wise operation is to mix the **filtered information** from each channel which is processed by different fixed filters. The targets of two the node-wise operations are actually different things.

- *FAGCN does not learn distinct information from different "channels". FAGCN only uses simple addition to mix information instead of node-wise channel mixing mechanism*

The learned filter \hat{A}' can be decomposed as $\hat{A}' = \hat{A}'_1 + (-\hat{A}'_2)$, where \hat{A}'_1 and $-\hat{A}'_2$ represent positive and negative edge (propagation) information, respectively. But FAGCN does not feed distinct information to \hat{A}'_1 and $-\hat{A}'_2$. Moreover, the aggregated $\hat{A}'_1 X$ and "diversified" information $(-\hat{A}'_2) X$ are simply added together instead of using any node-wise mixing mechanism. In ACM, we learn distinct information separately in each channel with different parameters and add them adaptively and node-wisely instead of just adding them together. In section 6.1, the ablation study has empirically shown that node-wise adaptive channel mixing is better than simple addition.